To: Mr. Chas. J. McCarthy

75

NATIONAL ADVISORY COMMITTEE FOR AERONAUTICS

SPECIAL REPORT 97

WIND-TUNNEL INVESTIGATION OF AN N.A.C.A. 23012 AIRFOIL WITH A SLOTTED FLAP AND THREE TYPES OF AUXILIARY FLAP

By Carl J. Wenzinger and William E. Gauvain
Langley Memorial Aeronautical Laboratory

December 1938

WIND-TUNNEL INVESTIGATION OF AN N.A.C.A. 23012 AIRFOIL WITH A SLOTTED FLAP AND THREE TYPES OF AUXILIARY FLAP

By Carl J. Wenzinger and William E. Gauvain

SUMMARY

An investigation was made in the N.A.C.A. 7- by 10-foot wind tunnel to determine the aerodynamic section characteristics of an N.A.C.A. 23012 airfoil with a single main slotted flap equipped successively with auxiliary flaps of the plain, split, and slotted types. A test installation was used in which an airfoil of 7-foot span was mounted vertically between the upper and the lower sides of the closed test section so that two-dimensional flow was approximated.

On the basis of maximum lift coefficient, low drag at moderate and high lift coefficients, and high drag at high lift coefficients, the optimum combination of the arrangements was found to be the double slotted flap. All the auxiliary flaps tested, however, increased the magnitudes of the pitching moments over those of the main slotted flap alone.

INTRODUCTION

Many different types of high-lift device have been investigated by the N.A.C.A. in an extensive program of research for increasing safety in flight. Some of these devices are located at the leading edge of the wing and others at the trailing edge. One of the most promising of the devices is a recently developed arrangement of slotted trailing-edge flap. This slotted flap (reference 1) is capable of giving high maximum lift coefficients, low drag at moderate and high lift coefficients, and high drag at high lift coefficients. This flap therefore appears well suited for improving take-off and landing characteristics.

Results of a few preliminary tests of a slotted flap with a small split flap mounted on it (reported also in reference 1) indicate that such an arrangement has considerable promise as a high-lift device. As a further development in enlarging the possibilities of the slotted flap, the investigation has been extended to include multiple flaps. The present report gives the results of an investigation of an airfoil with a medium-size main slotted flap combined with each of three different types of smaller auxiliary flap: split, plain, and slotted. Each of the auxiliary flaps was tested at a series of deflections for several deflections of the main flap. Measurements of lift, drag, and pitching moments were made in the 7- by 10-foot wind tunnel.

APPARATUS AND TESTS

Models

The basic model, or plain airfoil, was built to the N.A.C.A. 23012 profile and has a chord of 3 feet and a span of 7 feet. The solid nose piece was made of laminated mahogany, the ribs and the slot form were of pine, and the intermediate section was covered with tempered waterproofed wallboard. All the flaps were made of wood.

The main slotted flap has a chord 25.66 percent of the wing chord c_w; this flap together with its slot shape (fig. 1) is the same as the arrangement designated 2-h in reference 1. The flap was mounted on the airfoil with three fittings along the span that permitted setting the flap at the optimum location for each deflection. The ordinates for this flap and the slot shape are given in table I, and the optimum path of the nose of the flap for various deflections (from reference 1) is given in figure 2(a). The nose point of the flap is defined as the point of tangency of a line drawn normal to the airfoil chord and tangent to the leading-edge arc of the flap when neutral.

Two widths of split flap were tested: one has a chord $0.05c_w$ and the other a chord $0.10c_w$ (fig. 1). Each of these flaps was fastened to the lower surface of the main slotted flap by screws and blocks cut to different angles for the various flap deflections. The flap hinge axes were set in from the trailing edge of the main flap an amount equal to the chord of the split flaps.

The plain flap has a chord $0.10c_w$ and is formed from a portion of the main slotted flap, as shown in figure 1. This flap is arranged for locking at various angles, both up and down, with respect to the main flap. The gap between the plain-flap nose and the main slotted flap was sealed with a light grease for all tests to prevent leakage of air through the gap.

The auxiliary slotted flap (fig. 1) has a chord $0.10c_w$; the shapes of both the flap and the slot are similar to those of the main slotted flap. The ordinates for the auxiliary slotted flap and the slot shape are also given in table I. This flap was mounted on the main slotted flap by special fittings that allowed the small flap to be located at any point over a considerable area with respect to the main flap. This arrangement makes it possible to determine the optimum locations of the small slotted flap for the various deflections investigated. (See fig. 2(b).)

Test Installation

The model was mounted in the closed test section of the 7- by 10-foot wind tunnel so as to span the jet completely except for small clearances at each end. (See references 1 and 2.) The main airfoil was rigidly attached to the balance frame by torque tubes, which extended through the upper and the lower sides of the tunnel. The angle of attack of the model was set from outside the tunnel by rotating the torque tubes with a calibrated drive. Approximately two-dimensional flow is obtained with this type of installation and the section characteristics of the model under test can be determined. (See reference 1.)

Tests

All the tests were made at a dynamic pressure of 16.37 pounds per square foot, corresponding to an air speed of about 80 miles per hour at standard sea-level conditions. The average test Reynolds Number, based on the airfoil chord, was 2,190,000. This test Reynolds Number, when converted to an effective Reynolds Number that takes account of the turbulence in the air stream, is 3,500,000. (Effective Reynolds Number = average test Reynolds Number × turbulence factor; turbulence factor for the tunnel is 1.6.)

Tests were made of the airfoil with the main slotted flap first neutral and then deflected various amounts along the optimum flap path shown in figure 2(a). Each of the two auxiliary split flaps was next tested with deflections of 15°, 30°, 45°, and 60° for various deflections of the main slotted flap. Similar tests were then made of the auxiliary plain flap in combination with the main slotted flap.

The auxiliary slotted flap was deflected 10°, 20°, 30°, 40°, and 50° with the main slotted flap set neutral, and surveys were made to determine the optimum auxiliary-flap positions and deflections for maximum lift and steep angles of climb. Surveys were also made to determine whether these positions changed with deflection of the main slotted flap, but no surveys were made to determine whether the optimum path of the main slotted flap changed with deflection of the auxiliary flap. The optimum path finally chosen for the auxiliary slotted flap is shown in figure 2(b).

A sufficient number of angles of attack at each of the various deflections were investigated to determine envelope polars over the complete lift range from zero to maximum lift. Lift, drag, and pitching moments were measured for all positions of the flaps over the angle-of-attack range tested. No flap hinge moments or flap loads were obtained.

RESULTS AND DISCUSSION

Coefficients

All test results are given in standard section non-dimensional coefficient form as follows:

c_l, airfoil section lift coefficient (l/qS).

c_{d_o}, airfoil section drag coefficient (d_o/qS).

$c_{m_{(a.c.)_o}}$, airfoil section pitching-moment coefficient about aerodynamic center of section with flap in neutral position $(m/q\, c_w\, S)$.

where

l is the airfoil section lift.

d_o, airfoil section drag.

m, airfoil section pitching moment.

q, dynamic pressure $(\frac{1}{2}\rho V^2)$.

S, airfoil area including flap, measured with flap neutral.

c_w, airfoil chord.

and

δ_{f_1} is the setting of main slotted flap with respect to the airfoil, deg.

δ_{f_2}, setting of the auxiliary flap with respect to the main flap, deg.

α_o, angle of attack for infinite aspect ratio.

Precision

From repeat tests, the accidental experimental errors in the results presented herein are believed to lie within the following limits:

α - - - - - - - - - - - - - -	$\pm 0.25^\circ$
$c_{l_{max}}$ - - - - - - - - - - - -	± 0.03
$c_{m(a.c.)_o}$ - - - - - - - - - -	± 0.003
$c_{d_o(c_l=0)}$ - - - - - - - - - - -	± 0.0003
$c_{d_o(c_l=1.0)}$ - - - - - - - - - -	± 0.0006
$c_{d_o(c_l=2.5)}$ - - - - - - - - - -	± 0.002
Main-flap angle, δ_{f_1} - - - -	$\pm 0.3^\circ$
Main-flap position - - - - - -	$\pm 0.002c_w$
Auxiliary-flap angle, δ_{f_2} - -	$\pm 0.2^\circ$
Auxiliary-flap position - - - -	$\pm 0.001c_w$

The lift and the drag have been corrected for tunnel-wall effects, as explained in reference 1.

With certain arrangements of the main slotted flap with the auxiliary flap deflected, it was possible to obtain two sets of data, both of which are shown on the curves of section aerodynamic characteristics. Because of the innumerable possible combinations, the optimum nose path determined in reference 1 for the main flap was used. The slot opening for a main-flap deflection of approximately 30° in combination with some settings of the auxiliary flap seems to be critical since most of the double readings occurred with this arrangement. Undoubtedly, a more stable combination could have been found by adjusting the gap of the main flap but this procedure would have required more time than was available for these tests.

The profile-drag coefficient c_{d_o} of the airfoil-flap combinations has not been corrected for the effects of the various flap-hinge fittings. From previous tests of the airfoil with the main slotted flap (reference 1), it was found that the drag of the fittings did not exceed 0.001. The main-flap fittings used in the present tests were smaller than those mentioned and, as the auxiliary-flap fittings of the present model were small, it was estimated that their drag would not exceed 0.001.

Section Aerodynamic Characteristics

Main slotted flap.- The section aerodynamic characteristics of the airfoil with only the main slotted flap are included as a basis for comparison (fig. 3). The present data agree well with those given in reference 1, the chief difference being that the maximum lift is about 3 percent lower for the model used in these tests. This difference may be attributed to the use of an entirely different model and to slight differences in the accuracy of the flap setting.

Airfoil with main slotted flap and auxiliary split flaps.- Section aerodynamic characteristics of the airfoil with the slotted flap combined with the $0.05c_w$ split flap are given in figures 4 to 8, and envelope polar curves for this arrangement are plotted in figure 9. Similar data for the airfoil with the slotted flap and the $0.10c_w$ split flap are given in figures 10 to 15.

The envelope polar curves provide a convenient method for the comparison of the lift and the drag characteristics at various deflections of the combination of main and auxiliary flaps. Each envelope curve shows, for the combination being considered, the lowest drag obtainable at a given lift coefficient for a fixed deflection of the main flap. Figure 9 indicates that the $0.05c_w$ split flap will improve the effect of the main slotted flap alone for fixed main-flap deflections of 10°, 20°, 30°, and 40° when the split flap is deflected to give lift coefficients higher than 1.3, 1.6, 2.2, and 2.7. Similarly, figure 15 indicates that, for fixed main-flap deflections of 10°, 20°, 30°, and 40°, a beneficial effect will be obtained from the $0.10c_w$ split flap when it is deflected beyond the corresponding lift coefficients of 1.7, 2.2, 2.6, and 2.75.

<u>Airfoil with main slotted flap and auxiliary plain flap</u>.- Section aerodynamic characteristics of the airfoil with the main slotted flap combined with the $0.10c_w$ plain flap are given in figures 16 to 20, and envelope polar curves for the combination are plotted in figure 21. As for the combination of the slotted flap with the split flaps, some benefit is obtained. For fixed main-flap deflections of 10°, 20°, 30°, and 40°, figure 21 indicates that a beneficial effect will be obtained from the $0.10c_w$ plain flap when it is deflected at lift coefficients beyond 0.8, 1.95, 2.5, and 2.5.

<u>Airfoil with main slotted flap and auxiliary slotted flap</u>.- Section aerodynamic characteristics of the airfoil with the main slotted flap combined with the auxiliary $0.10c_w$ slotted flap are given in figures 22, 23, and 24, and envelope polar curves for the combination are plotted in figure 25. As previously mentioned, some preliminary tests were made to determine the optimum path of the auxiliary slotted flap for given deflections of the main flap; the optimum paths chosen are shown in figures 22, 23, and 24. A beneficial effect will be obtained from the auxiliary slotted flap for fixed main-flap deflections of 20° and 40° when the auxiliary flap is deflected at lift coefficients beyond 1.35 and 2.45.

Comparison of the Flap Arrangements Tested

An envelope of each of the series of envelope polar curves given in figures 9, 15, 21, and 25 has been plotted for each flap arrangement in figure 26. This figure shows that, from lift coefficients of 1.1 up to the stall, the lift and the drag characteristics of the airfoil with the main slotted flap can be improved by the addition of an auxiliary flap of the split or slotted type. The auxiliary plain flap offers an improvement over only two portions of the lift range, between $c_l = 1.1$ and 2.45 and from 2.73 to the stall. The superiority of the main slotted flap with the auxiliary slotted flap for high lift with low drag, which is very important for take-off and steep angles of climb, is immediately evident. High lift with high drag for landing purposes could be obtained by deflecting the slotted flaps to angles greater than 40°.

The various flap arrangements tested are also compared in table II. A comparison is made of the profile-drag coefficients at several different lift coefficients with the corresponding pitching moments and flap deflections; in the last two columns are given the ratio of lift to drag at maximum lift (an indication of the steepest gliding angle available), and the ratio of maximum lift to the drag at a lift coefficient of 0.2 (criterion of the speed range). The main slotted flap with the auxiliary slotted flap also shows up favorably in these comparisons, except as regards the pitching moments. For nearly all conditions, this combination has the highest pitching moments of the arrangements tested and this characteristic must be given consideration in applications to design.

The effect of the various flap arrangements in increasing the maximum lift of the airfoil is shown in figure 27 where values of the maximum-lift increment $\Delta c_{l_{max}}$ are plotted against deflections of the auxiliary flaps for given deflections of the main slotted flap. The superiority of the main slotted flap with the auxiliary slotted flap is immediately evident. It will be noted that, with the main slotted flap deflected 40° (its setting for $c_{l_{max}}$) and the auxiliary slotted flap deflected 30° or 40°, an increase of 1.46 in the maximum lift coefficient is possible. This increase almost doubles the maximum lift of the airfoil with flaps neutral, and still further increases might be expected with larger flaps and thicker airfoil sections. Further investigation along these lines is planned.

CONCLUSIONS

1. The optimum arrangement of the main and auxiliary flap combinations tested is the main slotted flap with the auxiliary slotted flap, which has more favorable characteristics than the single main slotted flap on the basis of maximum lift coefficient, low drag at moderate and high lift coefficients, and high drag at high lift coefficients.

2. The auxiliary split flap or the auxiliary plain flap combined with the main slotted flap slightly improves the aerodynamic characteristics at high lift coefficients.

3. All auxiliary flaps tested in combination with the main flap increase the magnitudes of the pitching moments over those of the main slotted flap alone.

Langley Memorial Aeronautical Laboratory,
National Advisory Committee for Aeronautics,
Langley Field, Va., October 31, 1938.

REFERENCES

1. Wenzinger, Carl J., and Harris, Thomas A.: Tests of an N.A.C.A. 23012 Airfoil with Various Arrangements of Slotted Flaps in the Closed-Throat 7- by 10-Foot Wind Tunnel. T.R. No. (to be published), N.A.C.A., 1939.

2. Harris, Thomas A.: The 7 by 10 Foot Wind Tunnel of the National Advisory Committee for Aeronautics. T.R. No. 412, N.A.C.A., 1931.

TABLE I

Ordinates for Flap and Slot Shapes

(Stations and ordinates in percent of airfoil chord)

Main slotted flap		
Station	Upper surface	Lower surface
0	-1.29	-1.29
.40	-.32	-2.05
.72	.04	-2.21
1.36	.61	-2.36
2.00	1.04	-2.41
2.64	1.40	-2.41
3.92	1.94	-
5.20	2.30	-
5.66	-	-2.16
6.48	2.53	-
7.76	2.63	-
9.03	2.58	-
10.31	2.46	-
15.66	1.68	-1.23
20.66	.92	-.70
25.66	.13	-.13
Center of leading-edge arc:		
0.91	-1.29	
Leading-edge radius: 0.91		

Contour of main slot	
Station	Ordinate
72.32	-1.02
74.57	.67
76.32	1.76
77.82	2.30
79.32	2.65
80.82	2.82
82.70	2.64
Center of arc:	
66.65	4.67
Radius of arc: 7.97	

Auxiliary slotted flap		
Station	Upper surface	Lower surface
0	-0.43	-0.43
.25	.06	-.84
.50	.31	-.92
.75	.49	-.98
1.00	.63	-1.00
1.50	.85	-1.02
2.00	.99	-1.00
2.50	1.08	-.96
3.00	1.12	-
3.50	1.12	-
4.00	1.06	-
Center of leading-edge arc:		
0.43	-0.43	
Leading-edge radius: 0.43		

Contour of auxiliary slot	
Station	Ordinate
89.50	-0.86
89	-.48
90	.28
90.50	.66
91	.90
91.50	1.05
92	1.17
92.50	1.22
93	1.15
93.23	1.13
Center of arc:	
89.59	1.52
Radius of arc: 3.05	

TABLE II

Comparison of Flap Arrangements Tested

c_l	c_{d_o}	$c_{m_{(a.c.)_o}}$	δ_{f_1} (deg.)	δ_{f_2} (deg.)	L/D at $c_{l_{max}}$	$\frac{c_{l_{max}}}{c_{d_o}(c_l=0.2)}$
Main slotted flap alone						
0	[a]0.0110	-0.010	0	-	21.00	237.4
1.0	.018	-.130	10	-		
		-.246	20	-		
1.5	.027	-.253	20	-		
2.0	.045	-.265	20	-		
			30	-		
2.5	.076	-.352	30	-		
[b]2.73	.13	-.370	40	-		
With auxiliary $0.10c_w$ plain flap						
0	[a]0.0114	-0.015	0	0	17.50	243.5
1.0	.018	-.240	20	0		
1.5	.026	-.250	20	0		
2.0	.042	-.367	30	0		
2.5	.079	-.345	30	0		
[b]2.80	.16	-.402	40	20		
With auxiliary $0.05c_w$ split flap						
0	[a]0.0110	-0.010	0	0	17.69	246.1
1.0	.018	-.130	10	0		
1.5	.027	-.253	20	0		
2.0	.045	-.306	20	15		
2.5	.073	-.448	30	30		
[b]2.83	.16	-.420	40	45		
With auxiliary $0.10c_w$ split flap						
0	[a]0.0110	-0.010	0	0	16.59	245.2
1.0	.018	-.130	10	0		
		-.245	20	0		
1.5	.027	-.253	20	0		
2.0	.046	-.247	20	0		
2.5	.076	-.353	30	0		
[b]2.82	.17	-.425	40	30		
With auxiliary $0.10c_w$ slotted flap						
0	[a]0.0118	-0.020	0	0	17.34	250.0
1.0	.018	-.245	20	0		
1.5	.026	-.348	20	10		
2.0	.039	-.424	20	20		
2.5	.066	-.400	20	20		
[b]3.00	.17	-.520	40	30		

[a]Minimum drag. [b]Maximum lift.

FIGURE LEGENDS

Figure 1.- Section view of the N.A.C.A. 23012 airfoil with the main slotted flap and the auxiliary flaps.

Figure 3.- Section characteristics of the N.A.C.A. 23012 airfoil with the main slotted flap deflected various amounts.

Figure 4.- Section characteristics of the N.A.C.A. 23012 airfoil with the main slotted flap deflected 0° and the auxiliary $0.05c_w$ split flap deflected various amounts.

Figure 5.- Section characteristics of the N.A.C.A. 23012 airfoil with the main slotted flap deflected 10° and the auxiliary $0.05c_w$ split flap deflected various amounts.

Figure 6.- Section characteristics of the N.A.C.A. 23012 airfoil with the main slotted flap deflected 20° and the auxiliary $0.05c_w$ split flap deflected various amounts.

Figure 7.- Section characteristics of the N.A.C.A. 23012 airfoil with the main slotted flap deflected 30° and the auxiliary $0.05c_w$ split flap deflected various amounts.

Figure 8.- Section characteristics of the N.A.C.A. 23012 airfoil with the main slotted flap deflected 40° and the auxiliary $0.05c_w$ split flap deflected various amounts.

Figure 9.- Envelope polar curves for the N.A.C.A. 23012 airfoil with the main slotted flap and the auxiliary $0.05c_w$ split flap.

Figure 10.- Section characteristics of the N.A.C.A. 23012 airfoil with the main slotted flap deflected 0° and the auxiliary $0.10c_w$ split flap deflected various amounts.

Figure 11.- Section characteristics of the N.A.C.A. 23012 airfoil with the main slotted flap deflected 10° and the auxiliary $0.10c_w$ split flap deflected various amounts.

Figure 12.- Section characteristics of the N.A.C.A. 23012 airfoil with the main slotted flap deflected 20° and the auxiliary $0.10c_w$ split flap deflected various amounts.

(a) Path of the main slotted flap for various deflections on the N.A.C.A. 23012 airfoil.

Path of flap nose for various flap deflections. Distances measured from lower edge of lip in percent airfoil chord, c_w.

δ_{f_1} (deg.)	x	y
0	8.36	3.91
10	5.41	3.63
20	3.83	3.45
30	2.63	3.37
40	1.35	2.43
50	.50	1.63
60	.12	1.48

(b) Path of the auxiliary $0.10c_w$ slotted flap for various deflections on the main slotted flap.

Path of flap nose for various flap deflections. Distances measured from lower edge of lip in percent airfoil chord, c_w.

δ_{f_1} (deg.)	δ_{f_2} (deg.)	x	y
0	0	3.22	1.58
20	10	1.55	1.52
20	20	1.32	1.50
20	30	1.06	1.50
40	20	.32	1.50
40	30	.06	1.27
40	40	.25	.59

Figure 2.- Optimum locations of the slotted flaps.

Figure 13.- Section characteristics of the N.A.C.A. 23012 airfoil with the main slotted flap deflected 30° and the auxiliary $0.10c_w$ split flap deflected various amounts.

Figure 14.- Section characteristics of the N.A.C.A. 23012 airfoil with the main slotted flap deflected 40° and the auxiliary $0.10c_w$ split flap deflected various amounts.

Figure 15.- Envelope polar curves for the N.A.C.A. 23012 airfoil with the main slotted flap and the auxiliary $0.10c_w$ split flap.

Figure 16.- Section characteristics of the N.A.C.A. 23012 airfoil with the main slotted flap deflected 0° and the auxiliary $0.10c_w$ plain flap deflected various amounts.

Figure 17.- Section characteristics of the N.A.C.A. 23012 airfoil with the main slotted flap deflected 10° and the auxiliary $0.10c_w$ plain flap deflected various amounts.

Figure 18.- Section characteristics of the N.A.C.A. 23012 airfoil with the main slotted flap deflected 20° and the auxiliary $0.10c_w$ plain flap deflected various amounts.

Figure 19.- Section characteristics of the N.A.C.A. 23012 airfoil with the main slotted flap deflected 30° and the auxiliary $0.10c_w$ plain flap deflected various amounts.

Figure 20.- Section characteristics of the N.A.C.A. 23012 airfoil with the main slotted flap deflected 40° and the auxiliary $0.10c_w$ plain flap deflected various amounts.

Figure 21.- Envelope polar curves for the N.A.C.A. 23012 airfoil with the main slotted flap and the auxiliary $0.10c_w$ plain flap.

δ_{f_2} (deg.)	x	y
0	3.22	1.58
10	.55	2.77
20	.32	2.50
30	.06	1.27
40	.25	.59
50	.42	.47

Optimum path of auxiliary flap nose for various flap deflections. Distances measured from lower edge of lip in percent of airfoil chord, c_w

Figure 22.- Section characteristics of the N.A.C.A. 23012 airfoil with the main slotted flap deflected 0° and the auxiliary $0.10c_w$ slotted flap deflected various amounts.

δ_{f_2} (deg.)	x	y
0	3.22	1.58
10	1.55	1.52
20	1.32	1.50
30	1.06	1.50
40	.75	.59
50	.42	.47

Optimum path of auxiliary flap nose for various flap deflections. Distances measured from lower edge of lip in percent of airfoil chord, c_w

Figure 23.- Section characteristics of the N.A.C.A. 23012 airfoil with the main slotted flap deflected 20° and the auxiliary $0.10c_w$ slotted flap deflected various amounts.

Optimum path of auxiliary flap nose for various flap deflections. Distances measured from lower edge of lip in percent of airfoil chord, c_w

δ_{f_2} (deg.)	x	y
0	3.22	1.58
10	.55	1.77
20	.32	1.50
30	.06	1.27
40	.25	.59

Figure 24.- Section characteristics of the N.A.C.A. 23012 airfoil with the main slotted flap deflected 40° and the auxiliary $0.10c_w$ slotted flap deflected various amounts.

Figure 25.- Envelope polar curves for the N.A.C.A. 23012 airfoil with the main slotted flap and the auxiliary $0.10c_w$ slotted flap.

Figure 26.- Envelope of envelope polar curves for the N.A.C.A. 23012 airfoil with the main slotted flap and various auxiliary flaps.

Figure 27.- Effect on section maximum-lift increment of various flap arrangements on the N.A.C.A. 23012 airfoil.

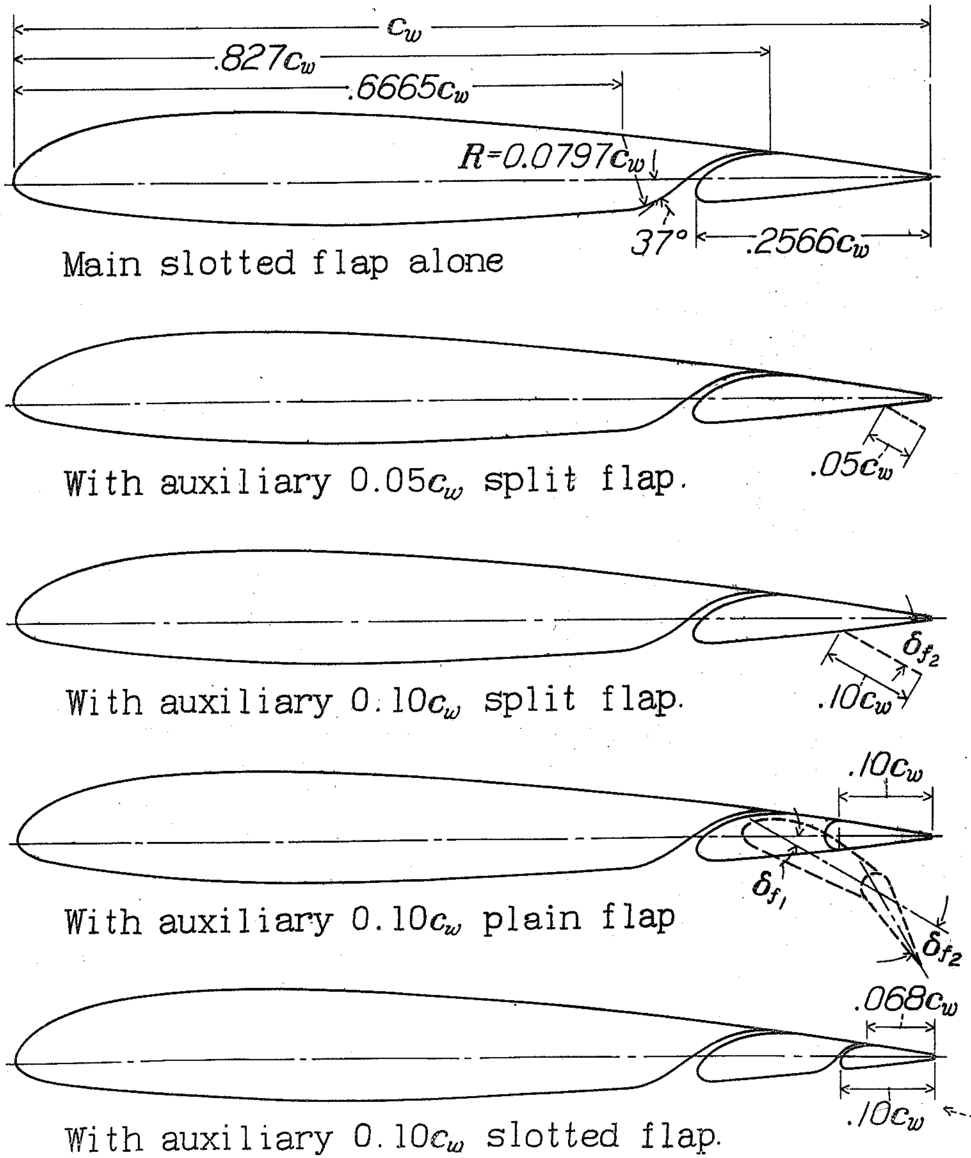

Figure 1.

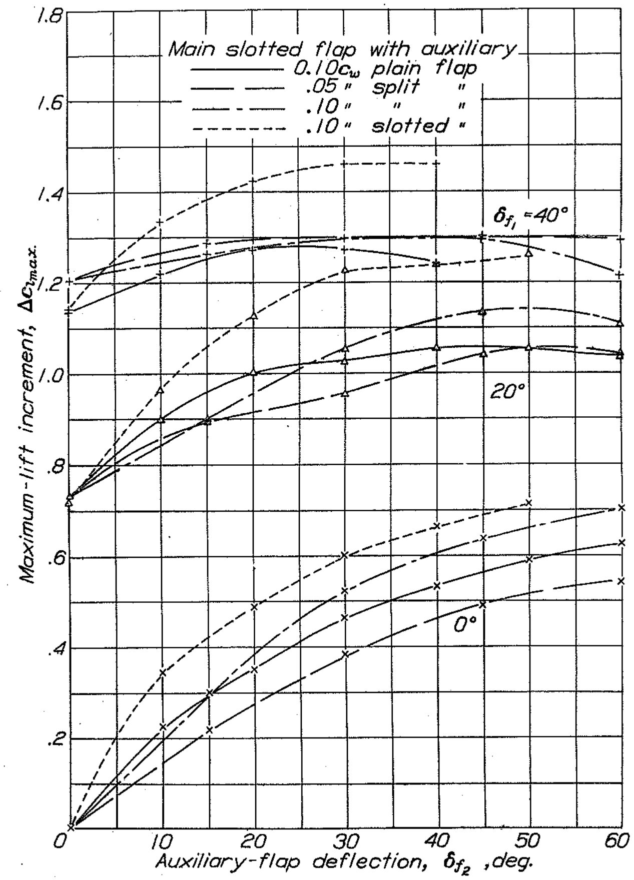

Figure 27.

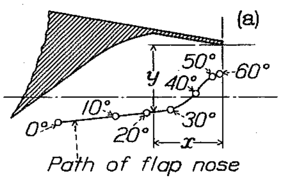

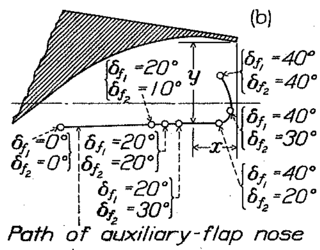

Figure 2

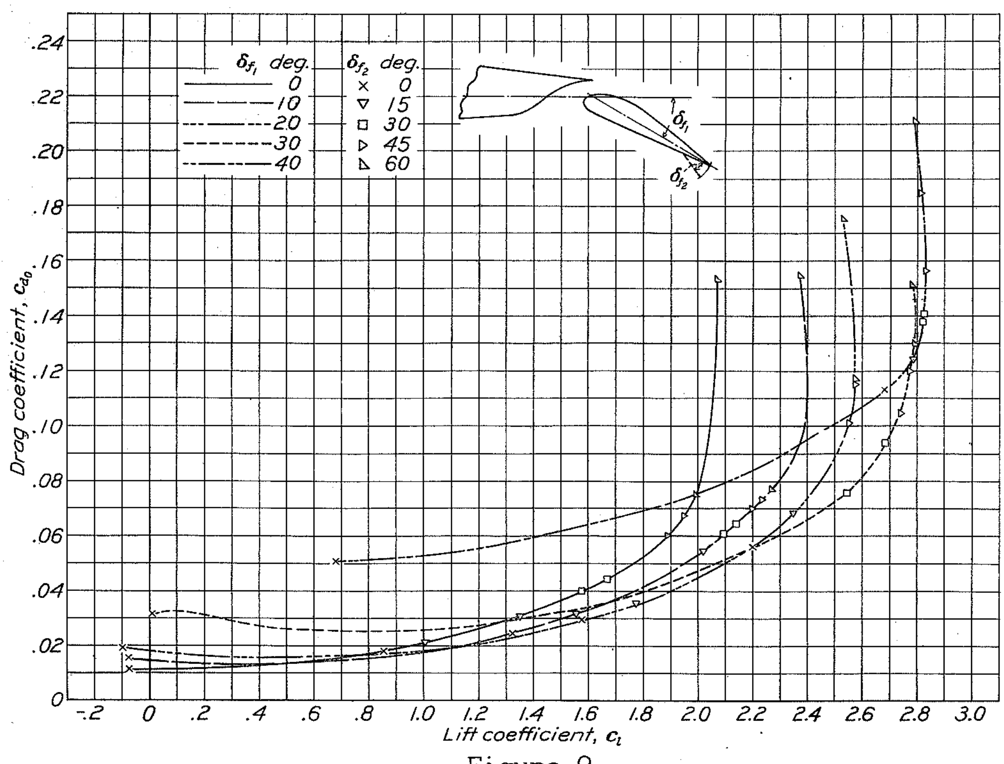

Figure 9

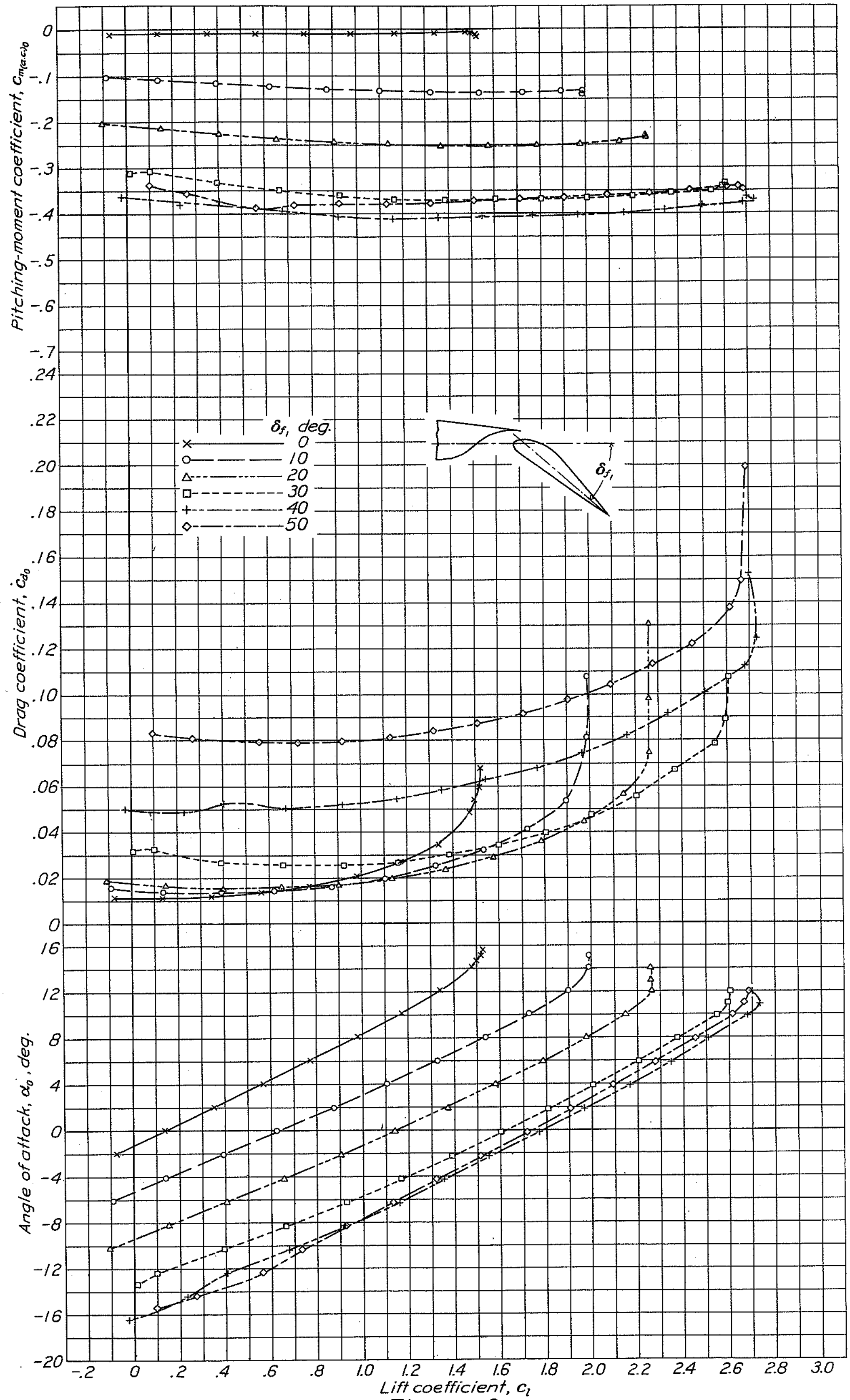
Pitching-moment coefficient, $c_{m_{(a.c.)_0}}$
Drag coefficient, c_{d_0}
Angle of attack, α_0, deg.
Lift coefficient, c_l
δ_{f_1}, deg.
0
10
20
30
40
50
δ_{f_1}

Figure 3

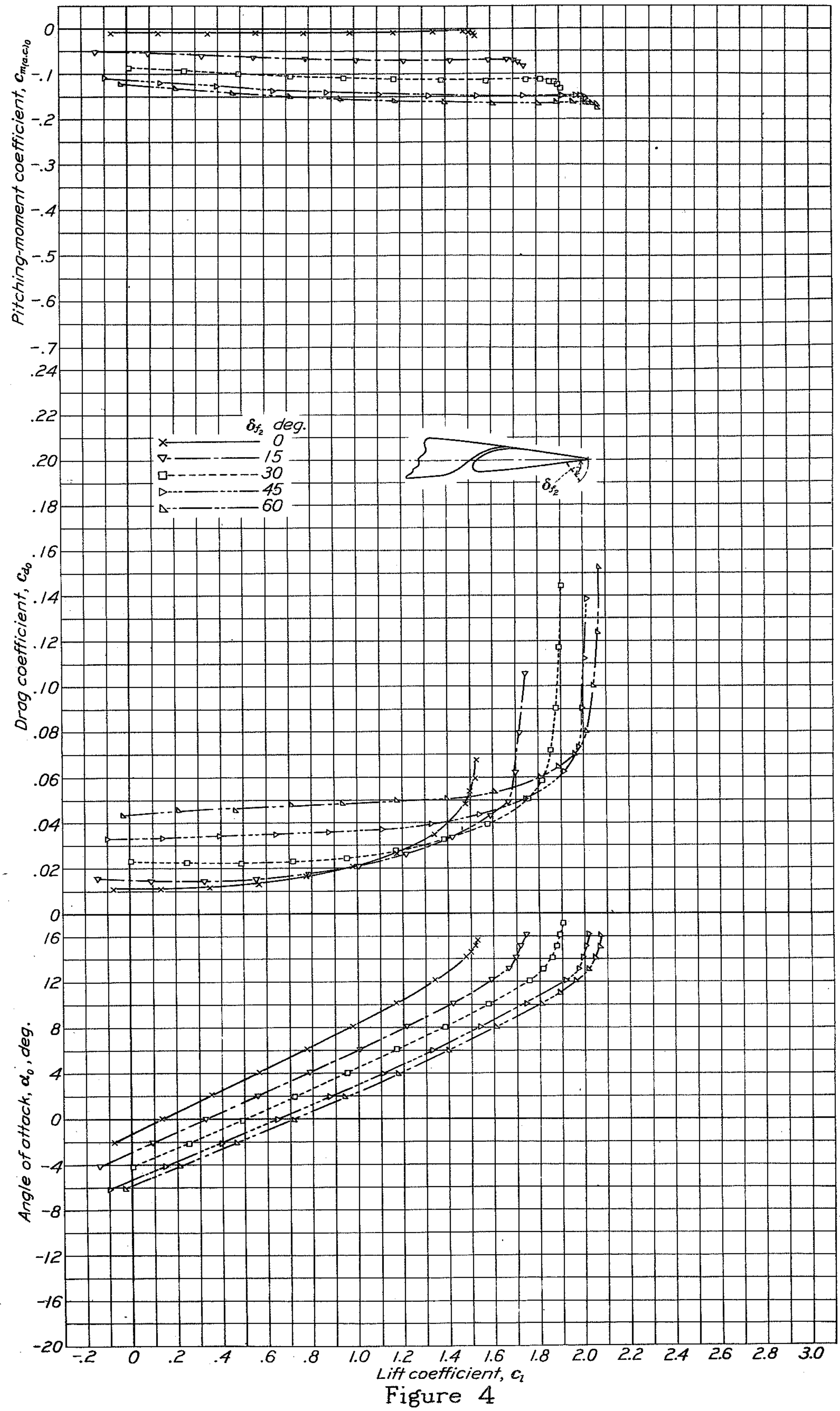
Pitching-moment coefficient, $c_{m(a.c.)_0}$
Drag coefficient, c_{d_0}
Angle of attack, α_0, deg.
Lift coefficient, c_l
δ_{f_2} deg.
0
15
30
45
60
δ_{f_2}

Figure 4

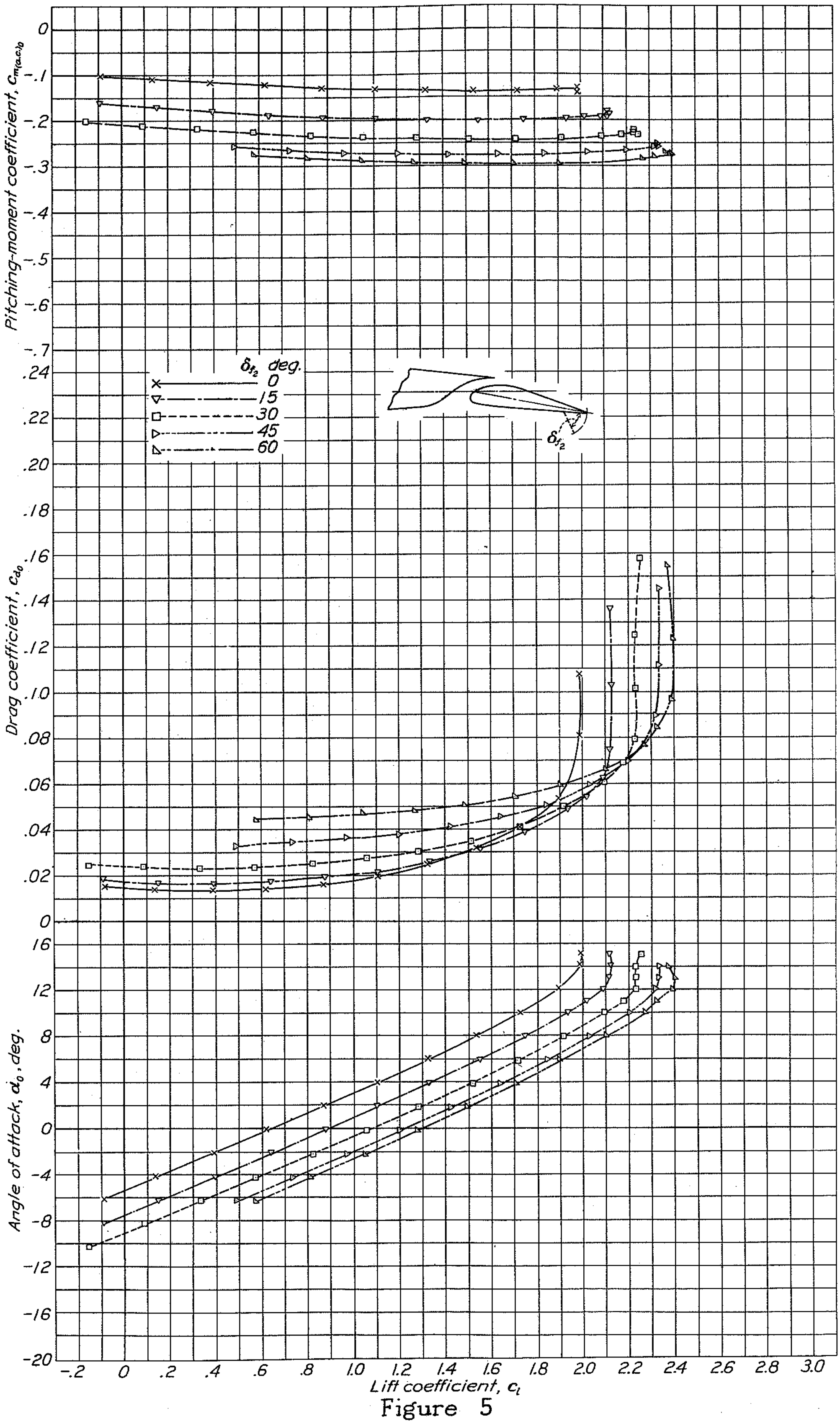
Pitching-moment coefficient, $c_{m_{(a.c.)_0}}$
0
-.1
-.2
-.3
-.4
-.5
-.6
-.7
δ_{f_2} deg.
0
15
30
45
60
δ_{f_2}
Drag coefficient, c_{d_0}
.24
.22
.20
.18
.16
.14
.12
.10
.08
.06
.04
.02
0
Angle of attack, α_0, deg.
16
12
8
4
0
-4
-8
-12
-16
-20
-.2 0 .2 .4 .6 .8 1.0 1.2 1.4 1.6 1.8 2.0 2.2 2.4 2.6 2.8 3.0
Lift coefficient, c_l

Figure 5

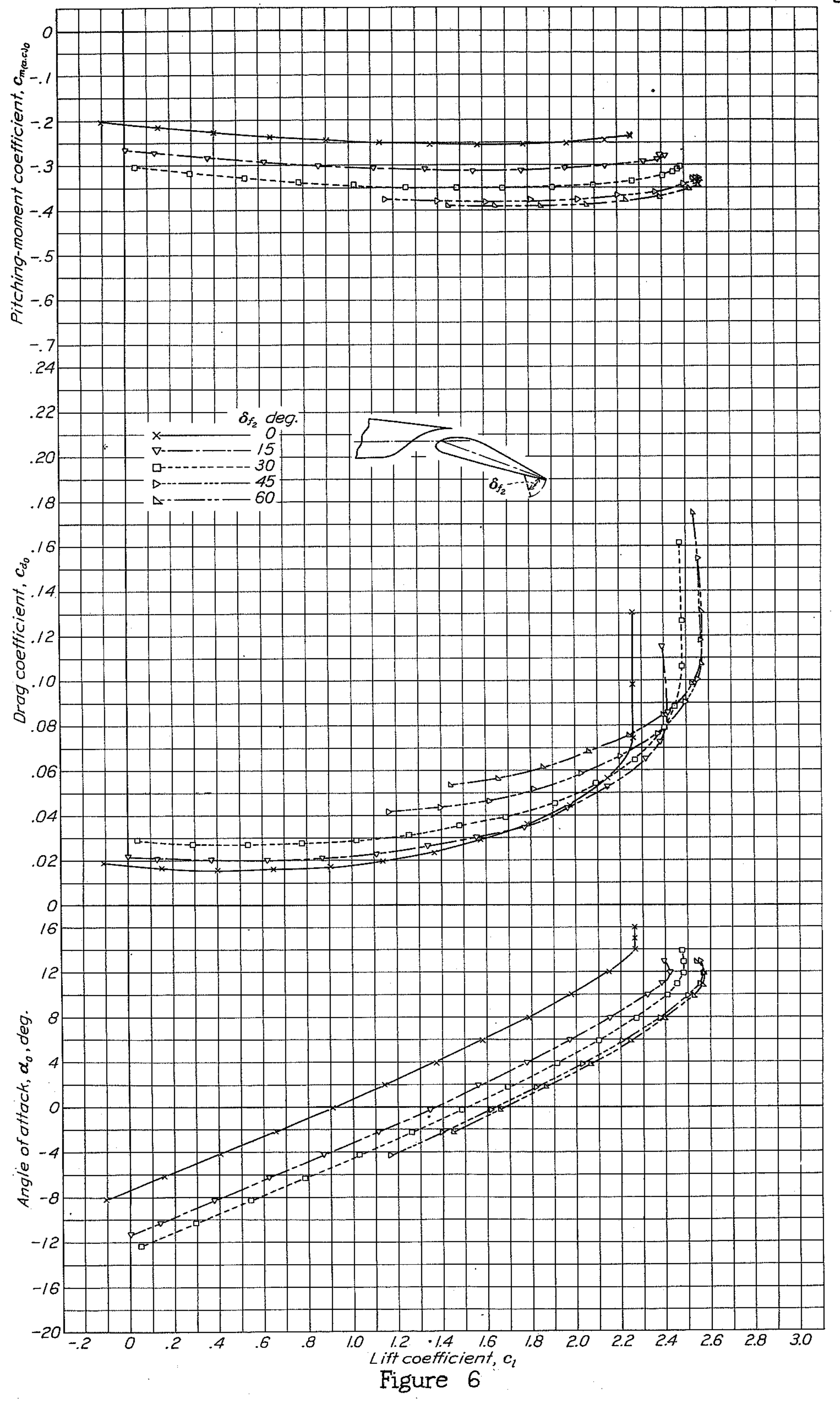
Pitching-moment coefficient, $c_{m(a.c.)_0}$
Drag coefficient, c_{d_0}
Angle of attack, α_0, deg.
Lift coefficient, c_l
δ_{f_2} deg.
0
15
30
45
60
δ_{f_2}
0
-.1
-.2
-.3
-.4
-.5
-.6
-.7
.24
.22
.20
.18
.16
.14
.12
.10
.08
.06
.04
.02
0
16
12
8
4
0
-4
-8
-12
-16
-20
-.2
0
.2
.4
.6
.8
1.0
1.2
1.4
1.6
1.8
2.0
2.2
2.4
2.6
2.8
3.0

Figure 6

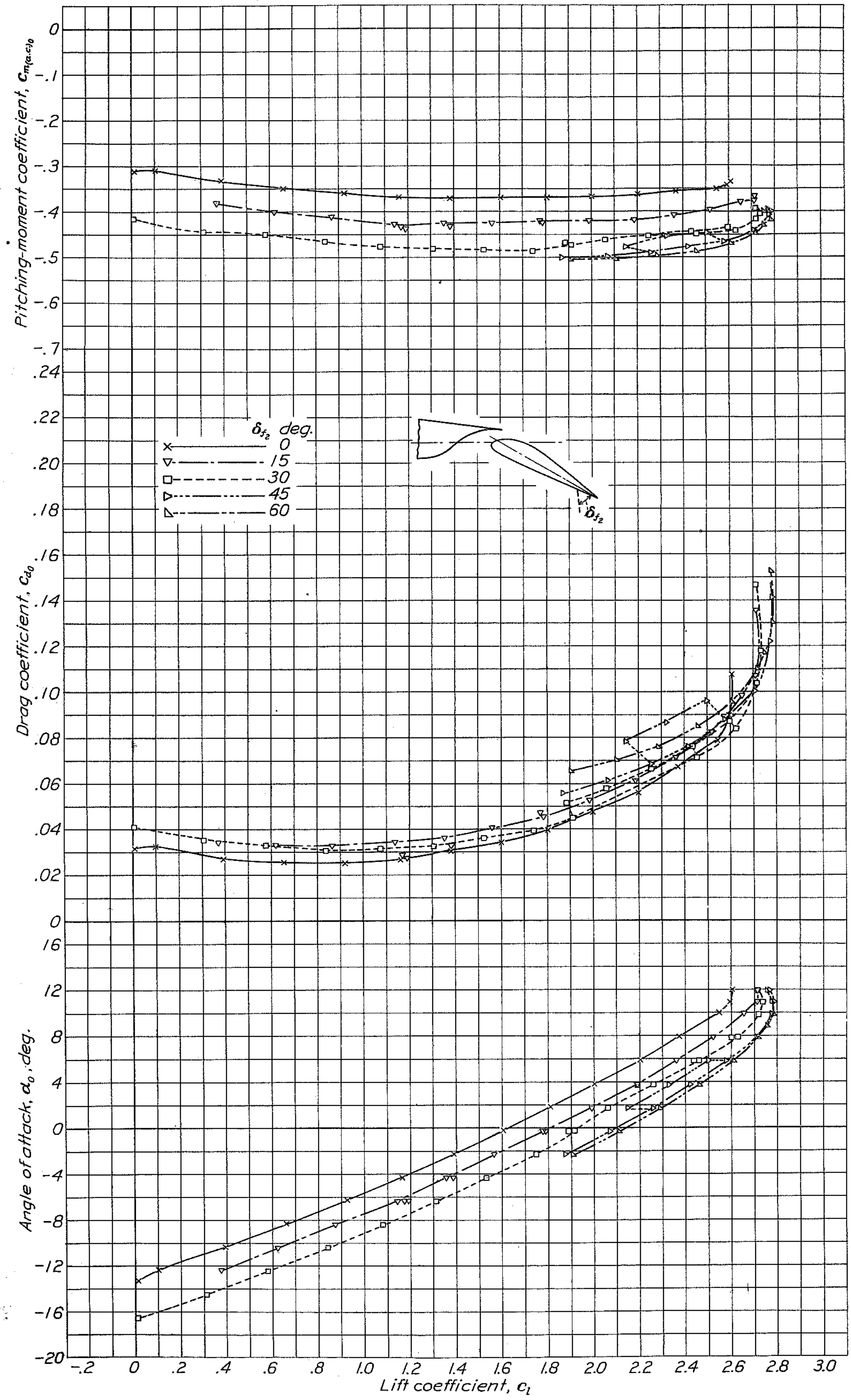
Pitching-moment coefficient, $c_{m(a.c.)_0}$
Drag coefficient, c_{d_0}
Angle of attack, α_0, deg.
Lift coefficient, c_l
δ_{f_2} deg.
0
15
30
45
60
δ_{f_2}

Figure 7

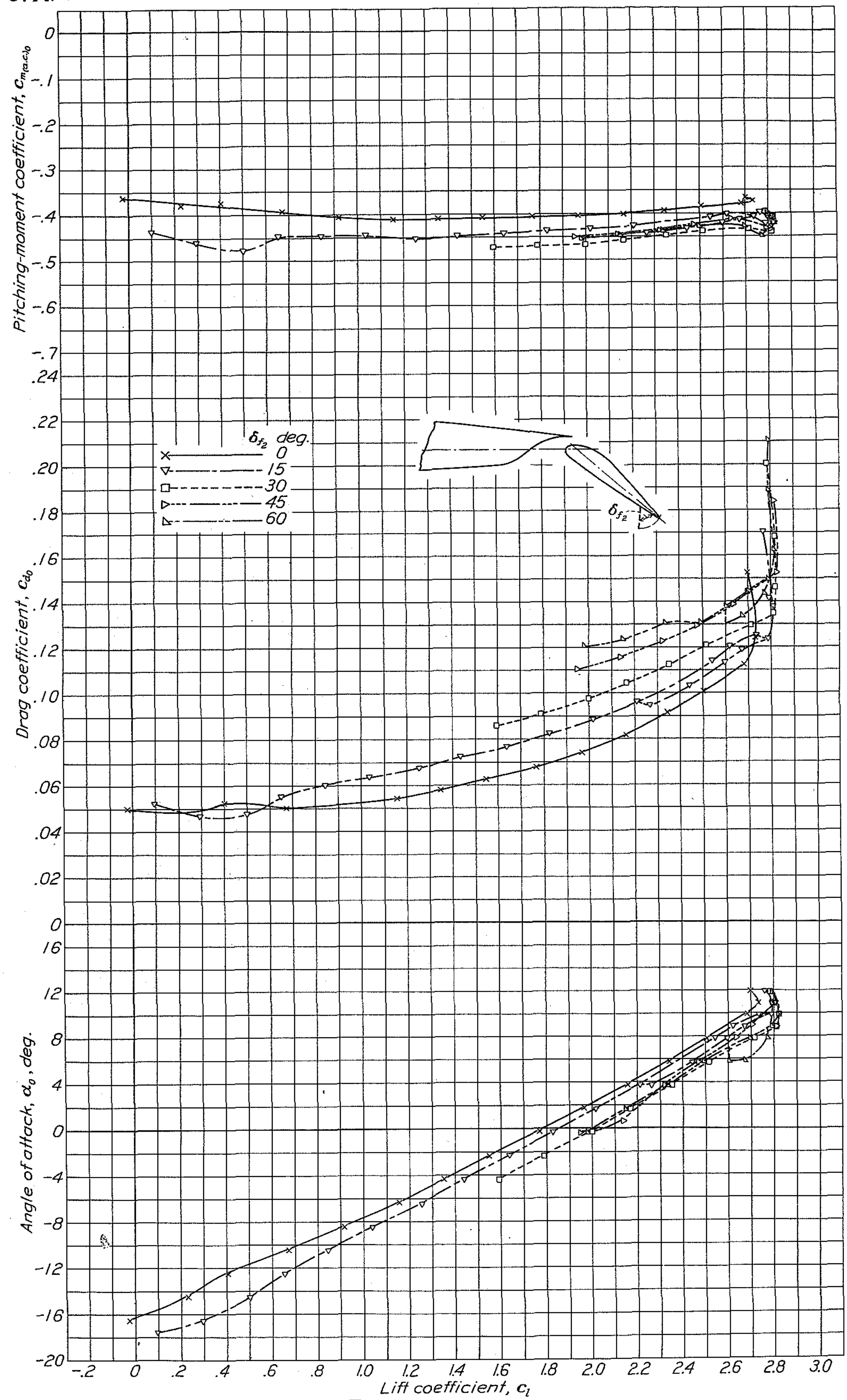
Pitching-moment coefficient, $c_{m_{(a.c.)_0}}$
0
-.1
-.2
-.3
-.4
-.5
-.6
-.7
Drag coefficient, c_{d_0}
.24
.22
.20
.18
.16
.14
.12
.10
.08
.06
.04
.02
0
δ_{f_2} deg.
0
15
30
45
60
δ_{f_2}
Angle of attack, α_0, deg.
16
12
8
4
0
-4
-8
-12
-16
-20
-.2
0
.2
.4
.6
.8
1.0
1.2
1.4
1.6
1.8
2.0
2.2
2.4
2.6
2.8
3.0
Lift coefficient, c_l

Figure 8

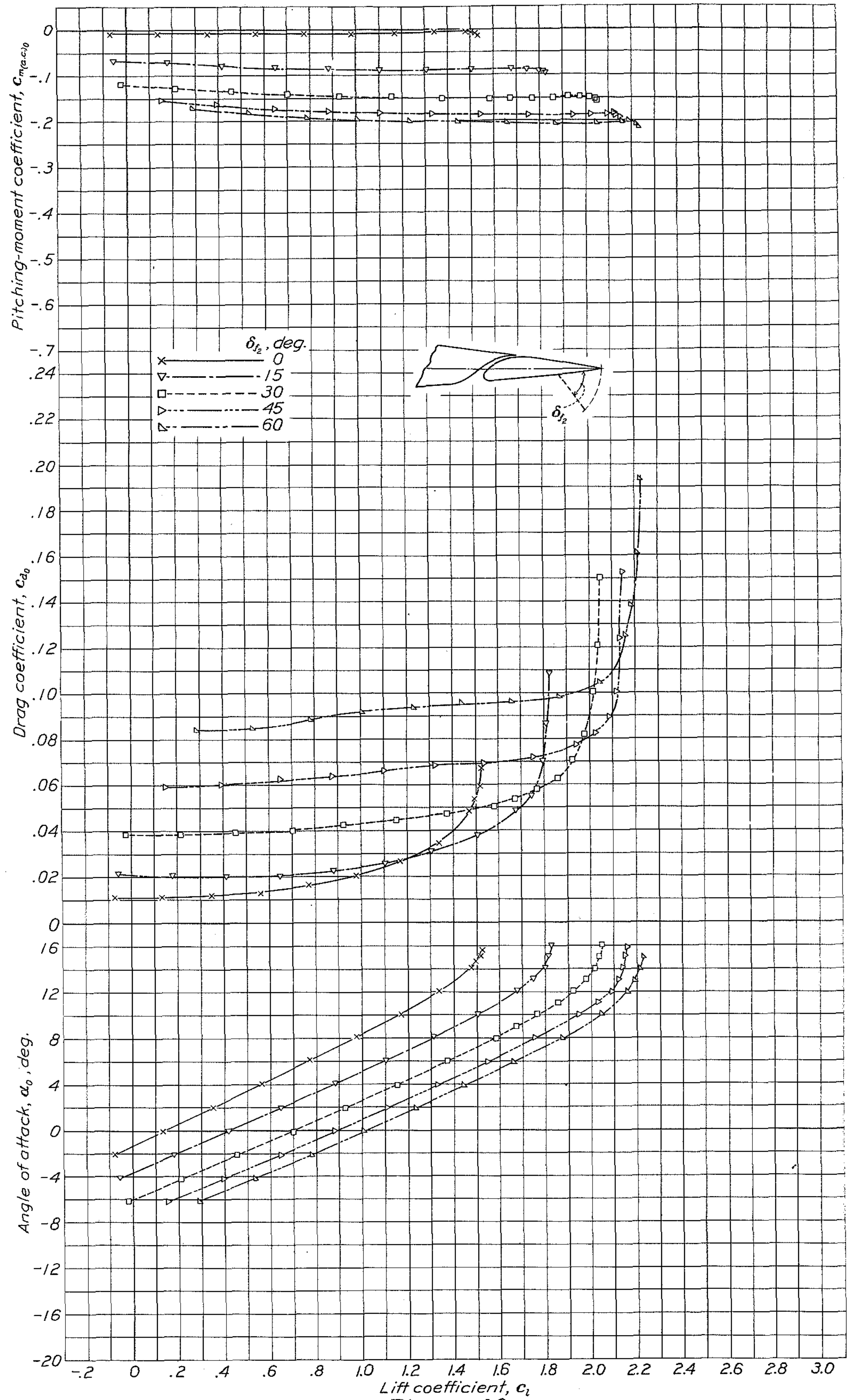

Pitching-moment coefficient, $c_{m_{(a.c.)_0}}$
Drag coefficient, c_{d_0}
Angle of attack, α_0, deg.
Lift coefficient, c_l
δ_{f_2}, deg.
0
15
30
45
60
δ_{f_2}

Figure 10

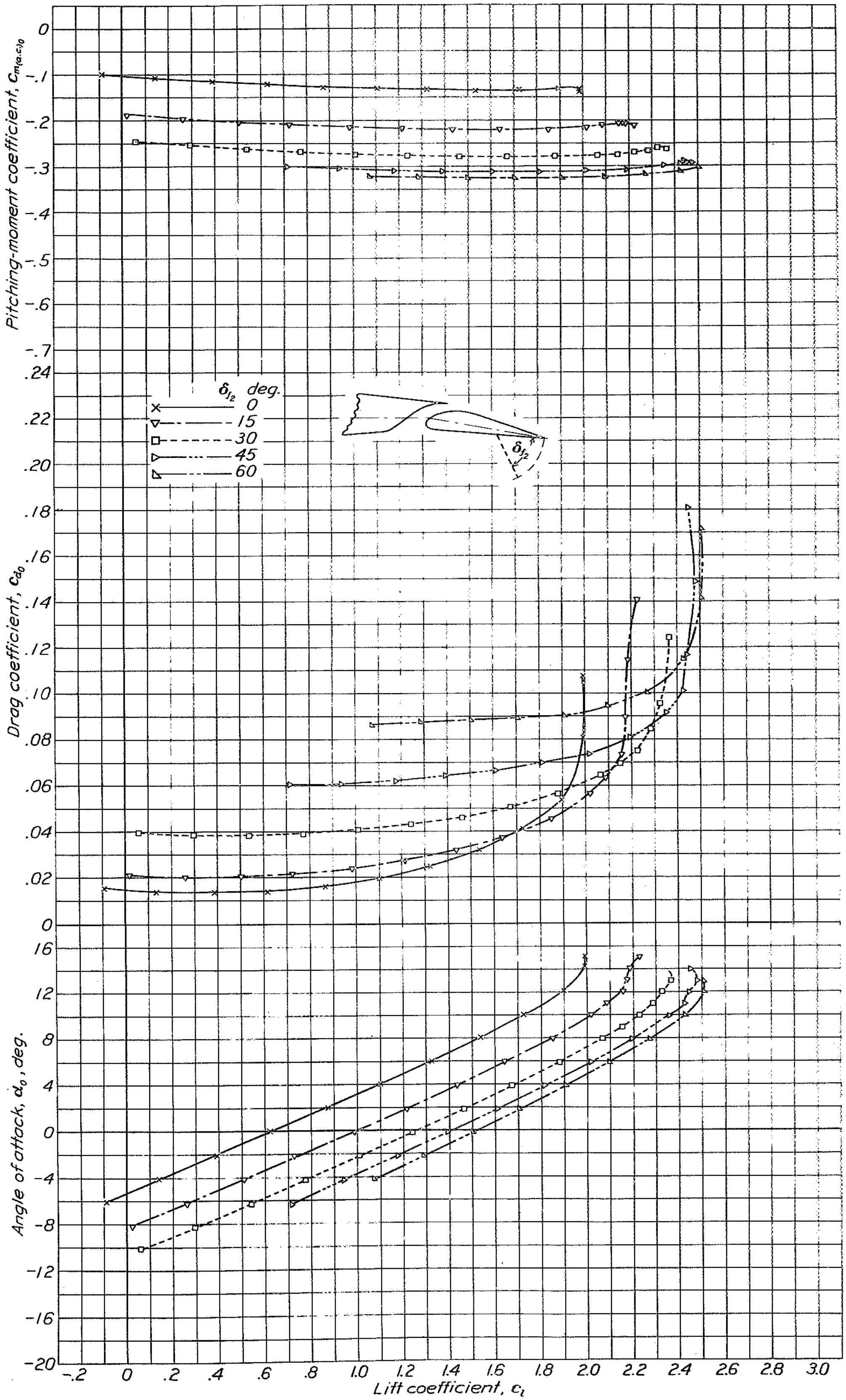
Pitching-moment coefficient, $c_{m_{(a.c.)_0}}$
Drag coefficient, c_{d_0}
Angle of attack, α_0, deg.
Lift coefficient, c_l
δ_{f_2} deg.
0
15
30
45
60
δ_{f_2}

Figure 11

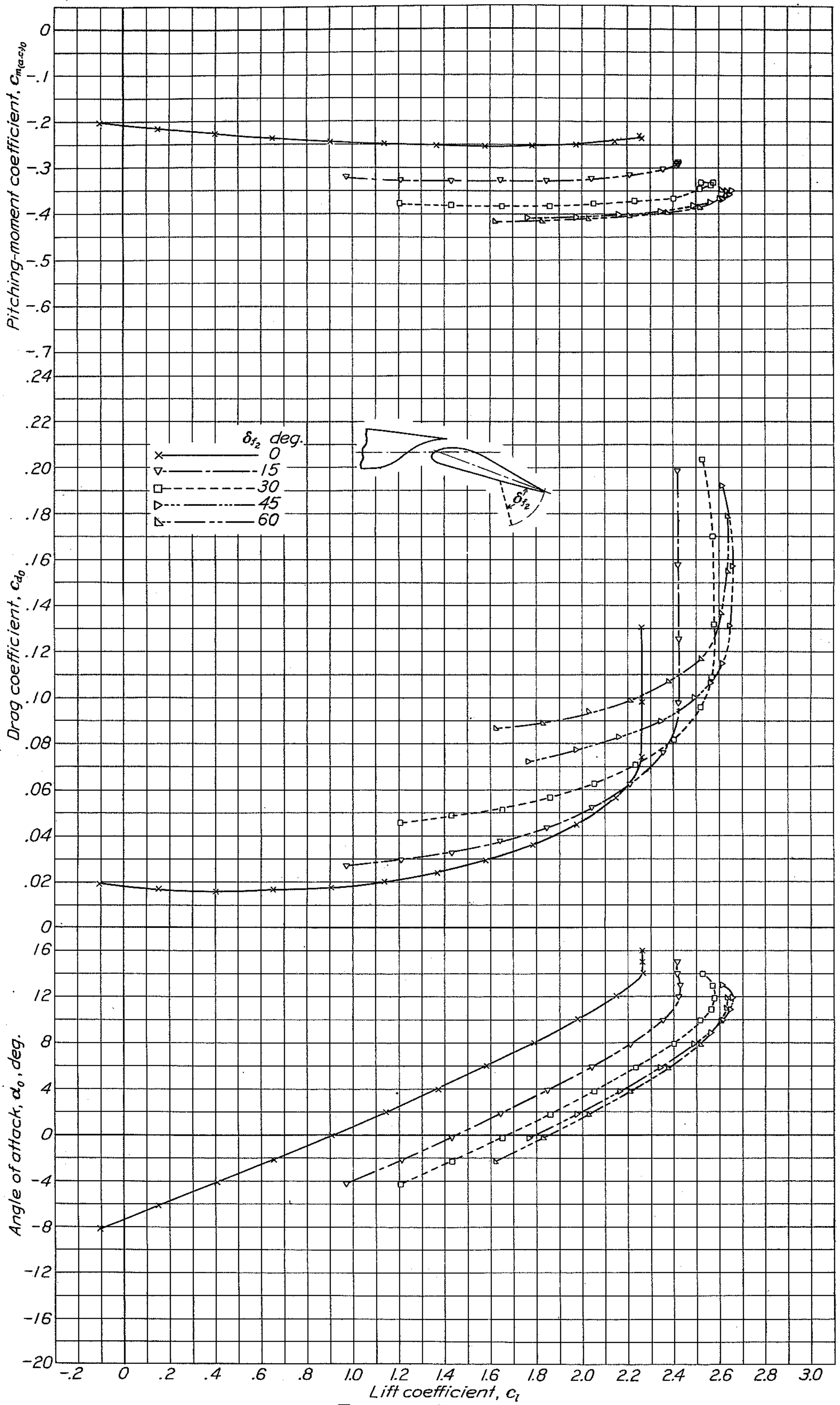
Pitching-moment coefficient, $c_{m_{(a.c.)_0}}$
Drag coefficient, c_{d_0}
Angle of attack, α_0, deg.
Lift coefficient, c_l
δ_{f_2} deg.
0
15
30
45
60
δ_{f_2}

Figure 12

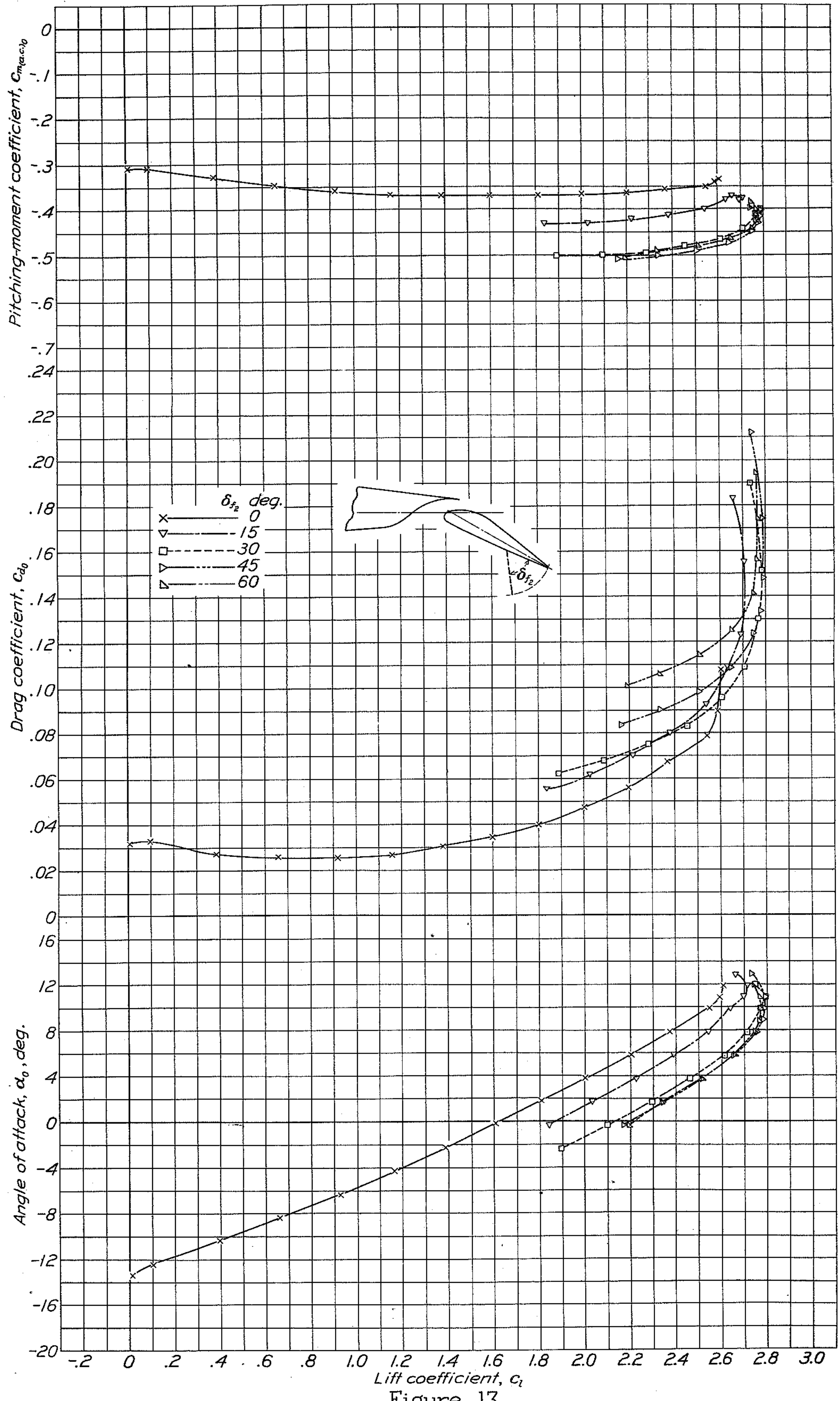
Pitching-moment coefficient, $c_{m_{(a.c.)_0}}$
Drag coefficient, c_{d_0}
Angle of attack, α_0, deg.
δ_{f_2} deg.
0
15
30
45
60
δ_{f_2}
Lift coefficient, c_l

Figure 13

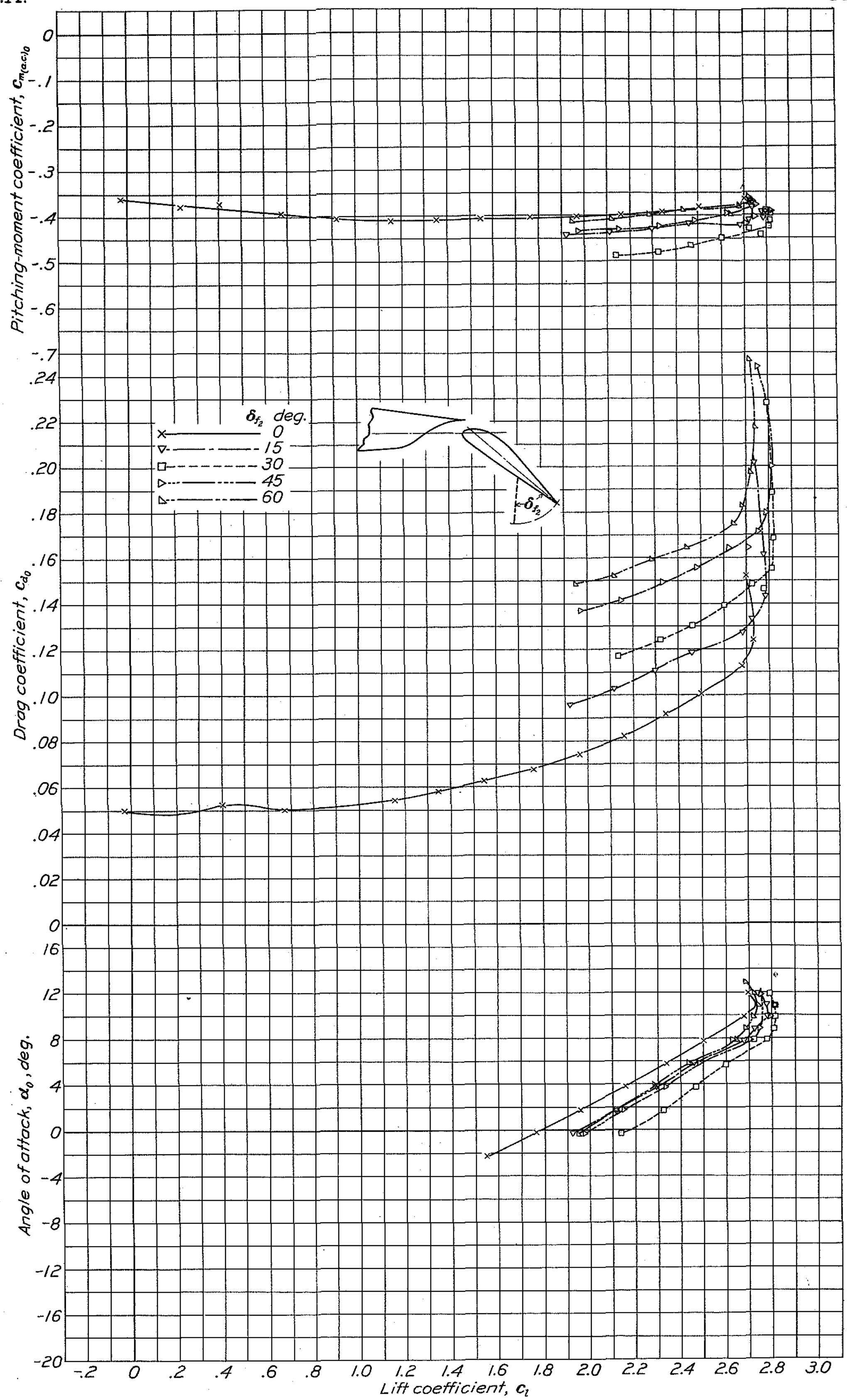
Pitching-moment coefficient, $c_{m_{(a.c.)_0}}$
0
-.1
-.2
-.3
-.4
-.5
-.6
-.7
Drag coefficient, c_{d_0}
.24
.22
.20
.18
.16
.14
.12
.10
.08
.06
.04
.02
0
Angle of attack, α_0, deg.
16
12
8
4
0
-4
-8
-12
-16
-20
δ_{f_2} deg.
0
15
30
45
60
δ_{f_2}
-.2
0
.2
.4
.6
.8
1.0
1.2
1.4
1.6
1.8
2.0
2.2
2.4
2.6
2.8
3.0
Lift coefficient, c_l

Figure 14

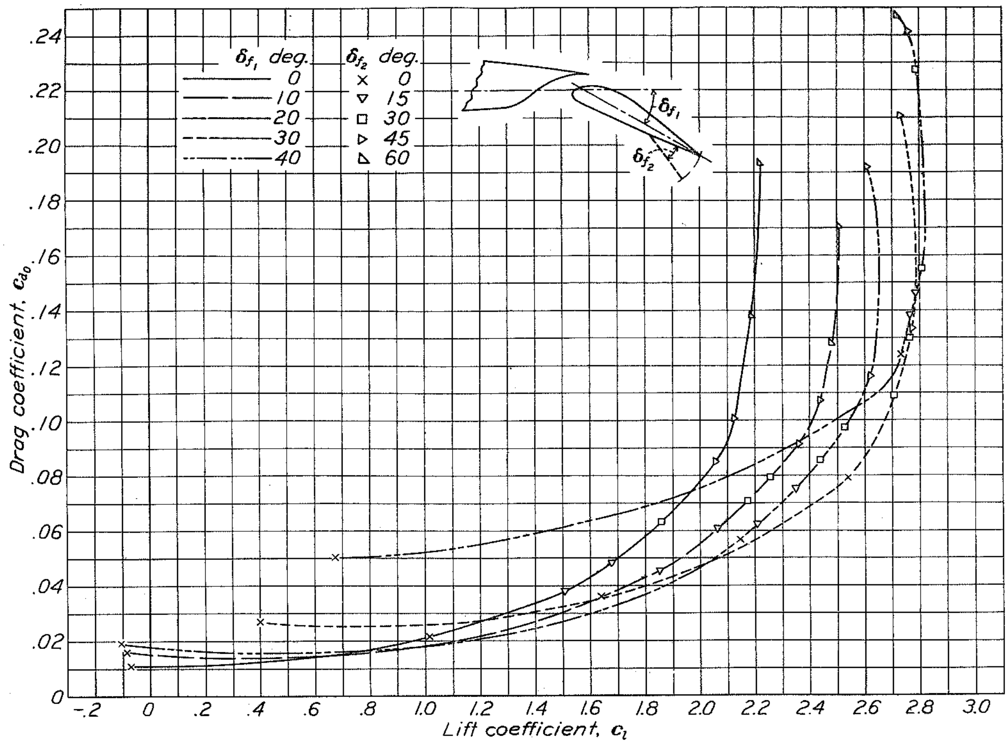

Figure 15

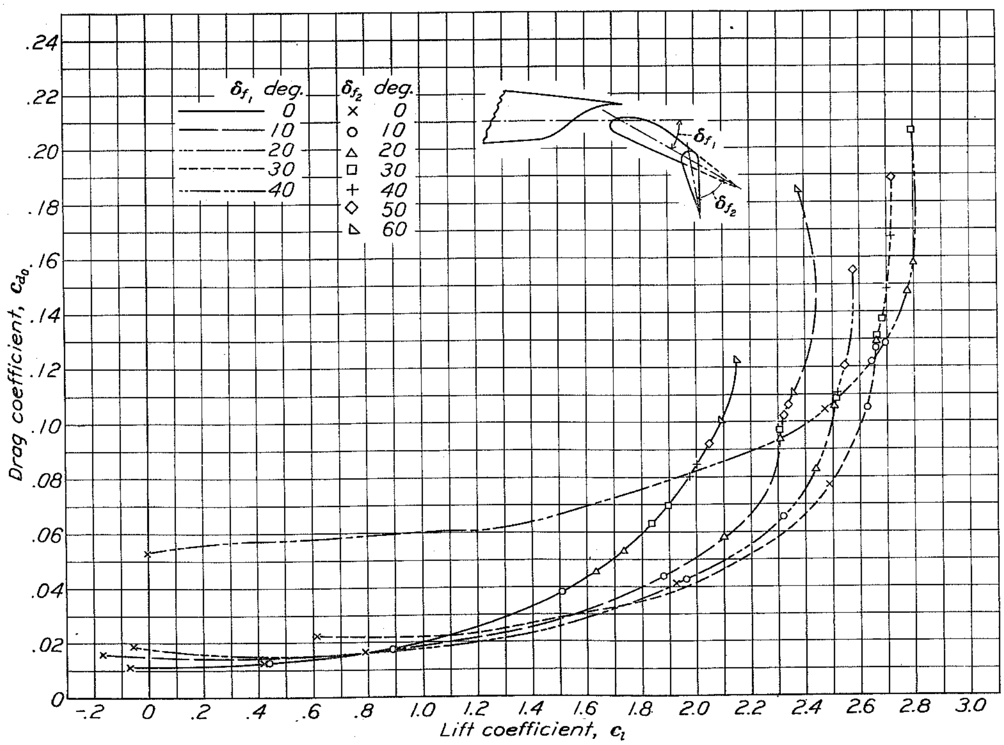

Figure 21

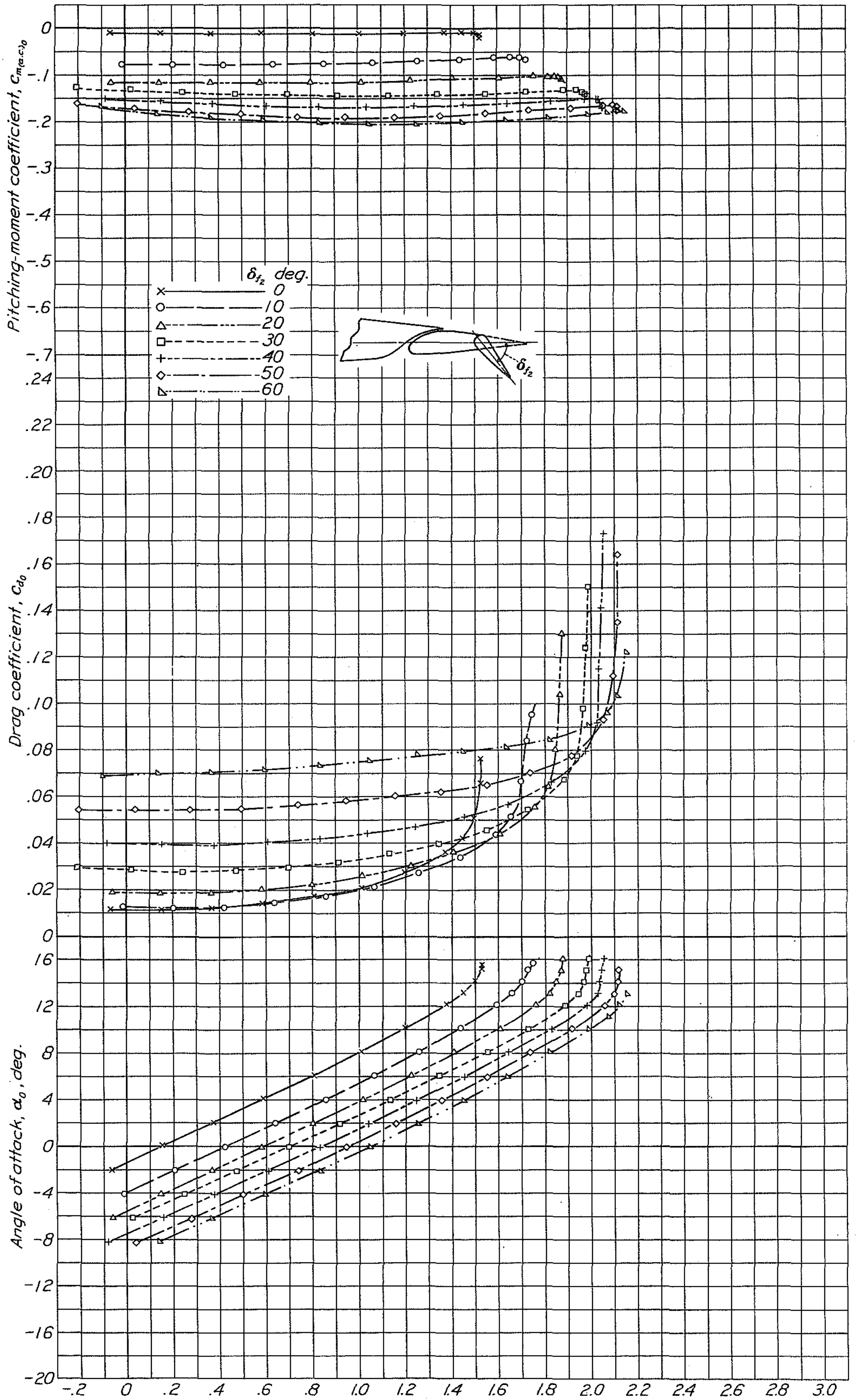
Pitching-moment coefficient, $c_{m_{(a.c.)_0}}$
Drag coefficient, c_{d_0}
Angle of attack, α_0, deg.
Lift coefficient, c_l
δ_{f_2} deg.
0
10
20
30
40
50
60
δ_{f_2}
0
-.1
-.2
-.3
-.4
-.5
-.6
-.7
.24
.22
.20
.18
.16
.14
.12
.10
.08
.06
.04
.02
0
16
12
8
4
0
-4
-8
-12
-16
-20
-.2
0
.2
.4
.6
.8
1.0
1.2
1.4
1.6
1.8
2.0
2.2
2.4
2.6
2.8
3.0

Figure 16

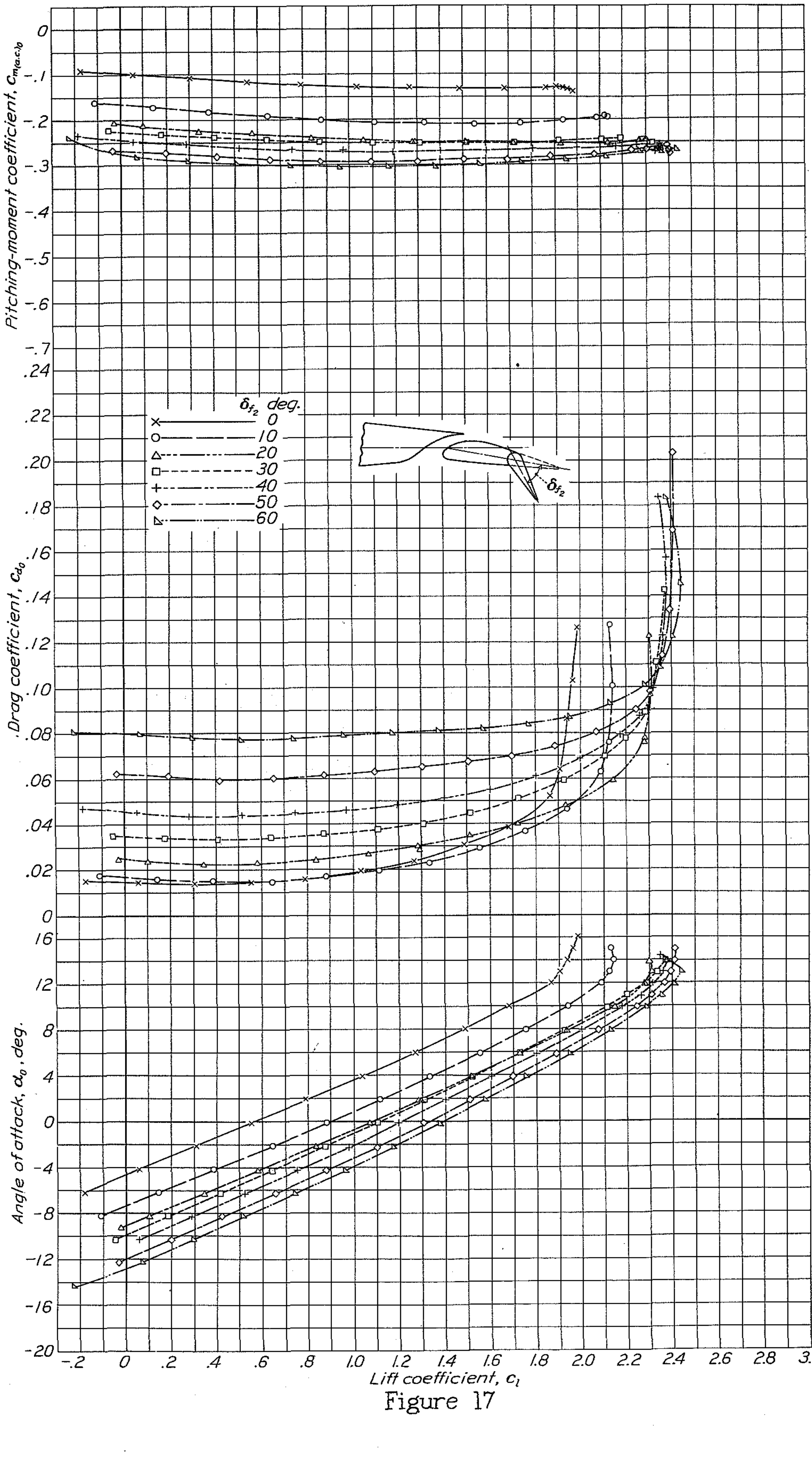
Pitching-moment coefficient, $c_{m(a.c.)_0}$
Drag coefficient, c_{d_0}
Angle of attack, α_0, deg.
Lift coefficient, c_l
δ_{f_2} deg.
0
10
20
30
40
50
60
δ_{f_2}
0
-.1
-.2
-.3
-.4
-.5
-.6
-.7
.24
.22
.20
.18
.16
.14
.12
.10
.08
.06
.04
.02
0
16
12
8
4
0
-4
-8
-12
-16
-20
-.2
0
.2
.4
.6
.8
1.0
1.2
1.4
1.6
1.8
2.0
2.2
2.4
2.6
2.8
3.0

Figure 17

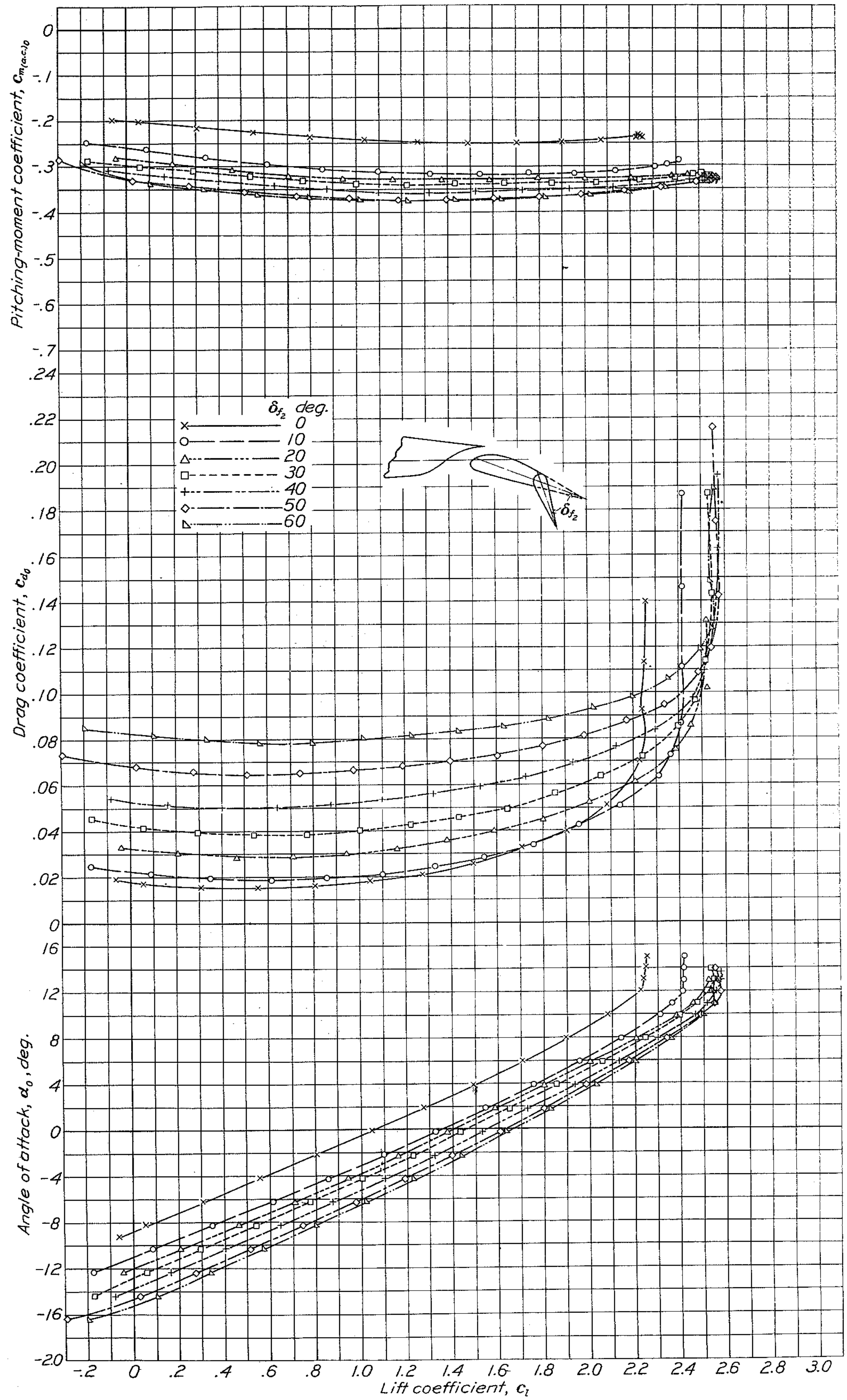
Pitching-moment coefficient, $c_{m_{(a.c.)_0}}$
0
-.1
-.2
-.3
-.4
-.5
-.6
-.7
Drag coefficient, c_{d_0}
.24
.22
.20
.18
.16
.14
.12
.10
.08
.06
.04
.02
0
δ_{f_2} deg.
0
10
20
30
40
50
60
δ_{f_2}
Angle of attack, α_0, deg.
16
12
8
4
0
-4
-8
-12
-16
-20
-.2
0
.2
.4
.6
.8
1.0
1.2
1.4
1.6
1.8
2.0
2.2
2.4
2.6
2.8
3.0
Lift coefficient, c_l

Figure 18

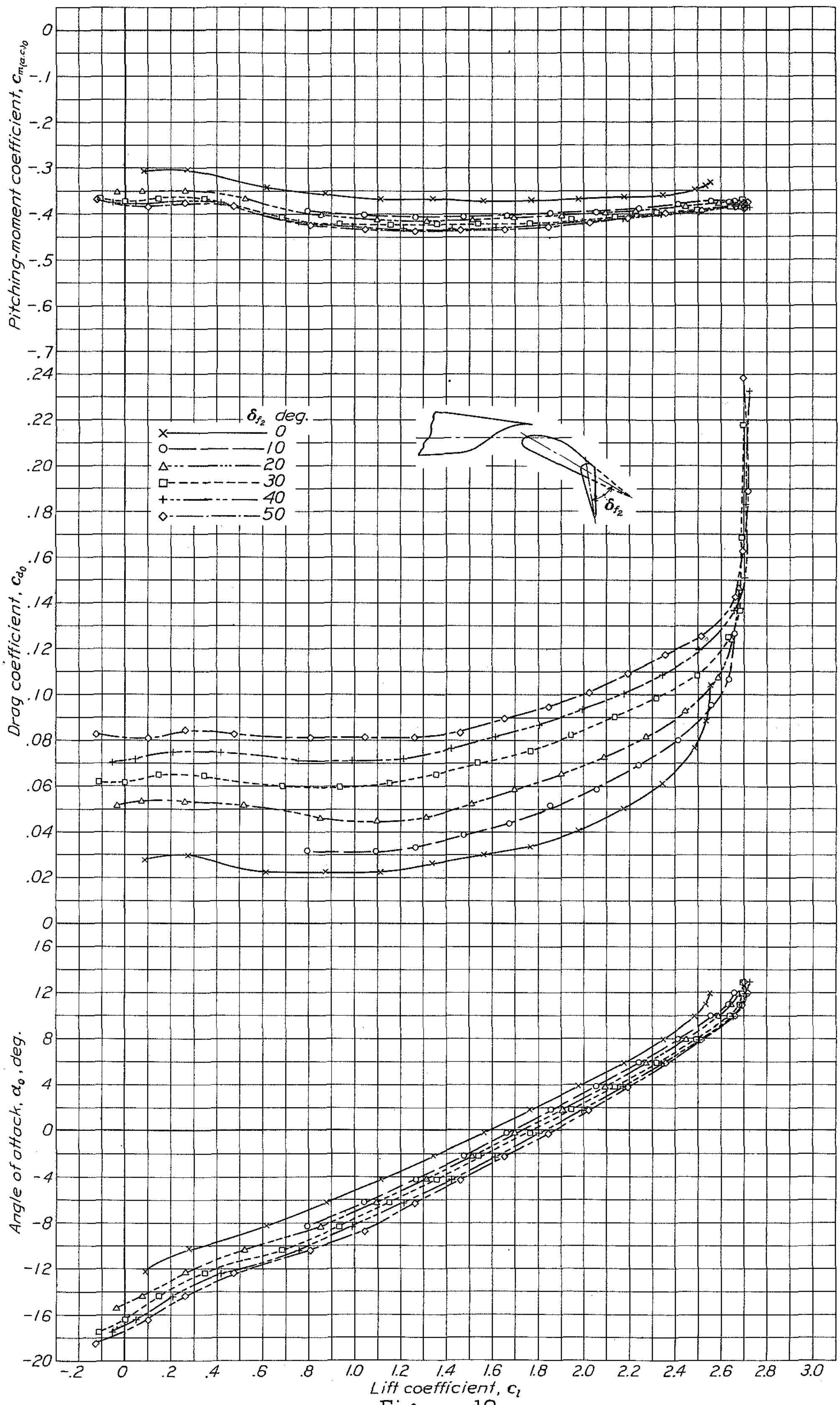
Pitching-moment coefficient, $c_{m(a.c.)_0}$
Drag coefficient, c_{d_0}
Angle of attack, α_0, deg.
Lift coefficient, c_l
δ_{f_2} deg.
0
10
20
30
40
50
δ_{f_2}

Figure 19

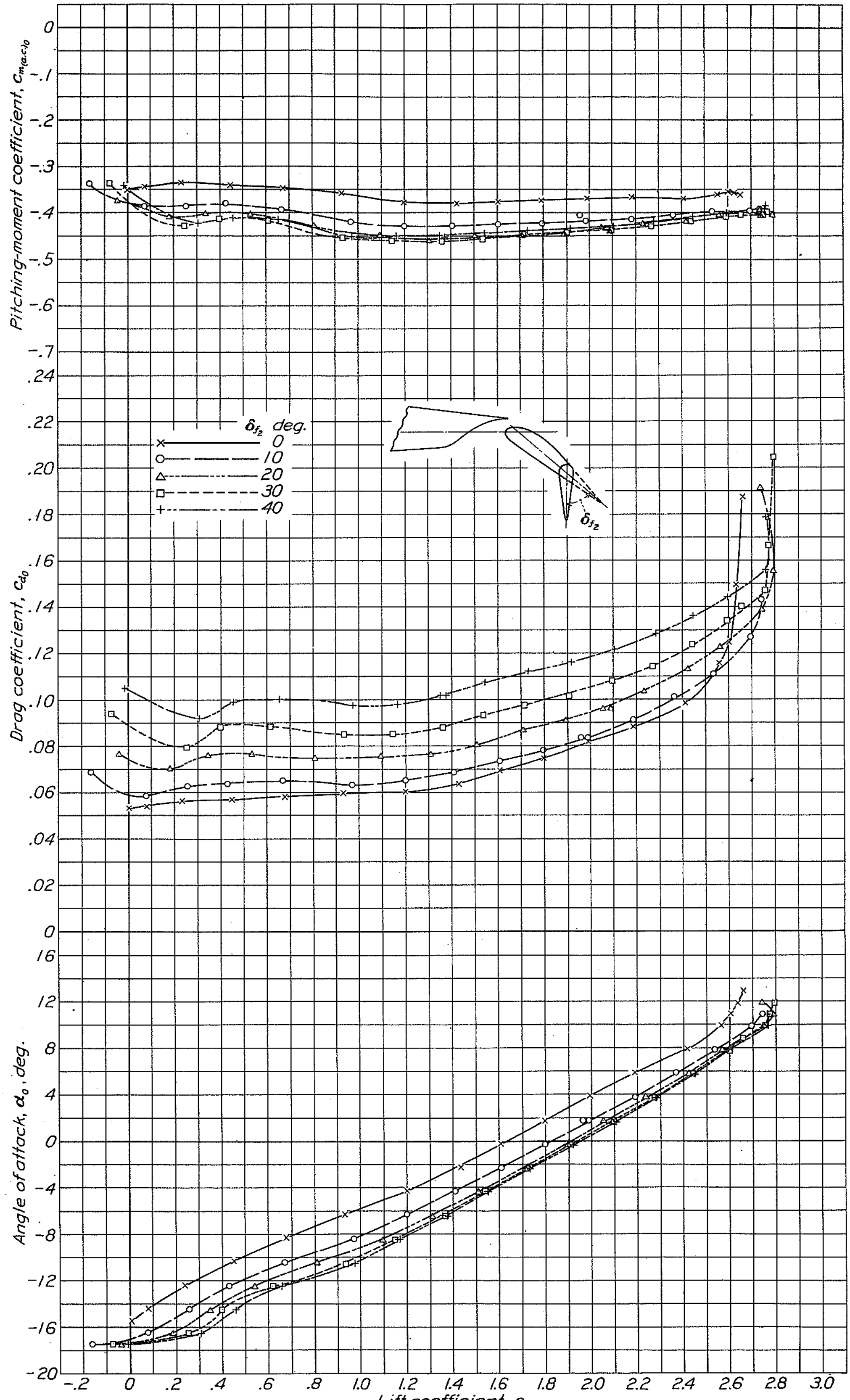
Pitching-moment coefficient, $c_{m_{(a.c.)_0}}$
Drag coefficient, c_{d_0}
Angle of attack, α_0, deg.
Lift coefficient, c_l
δ_{f_2} deg.
0
10
20
30
40
δ_{f_2}

Figure 20

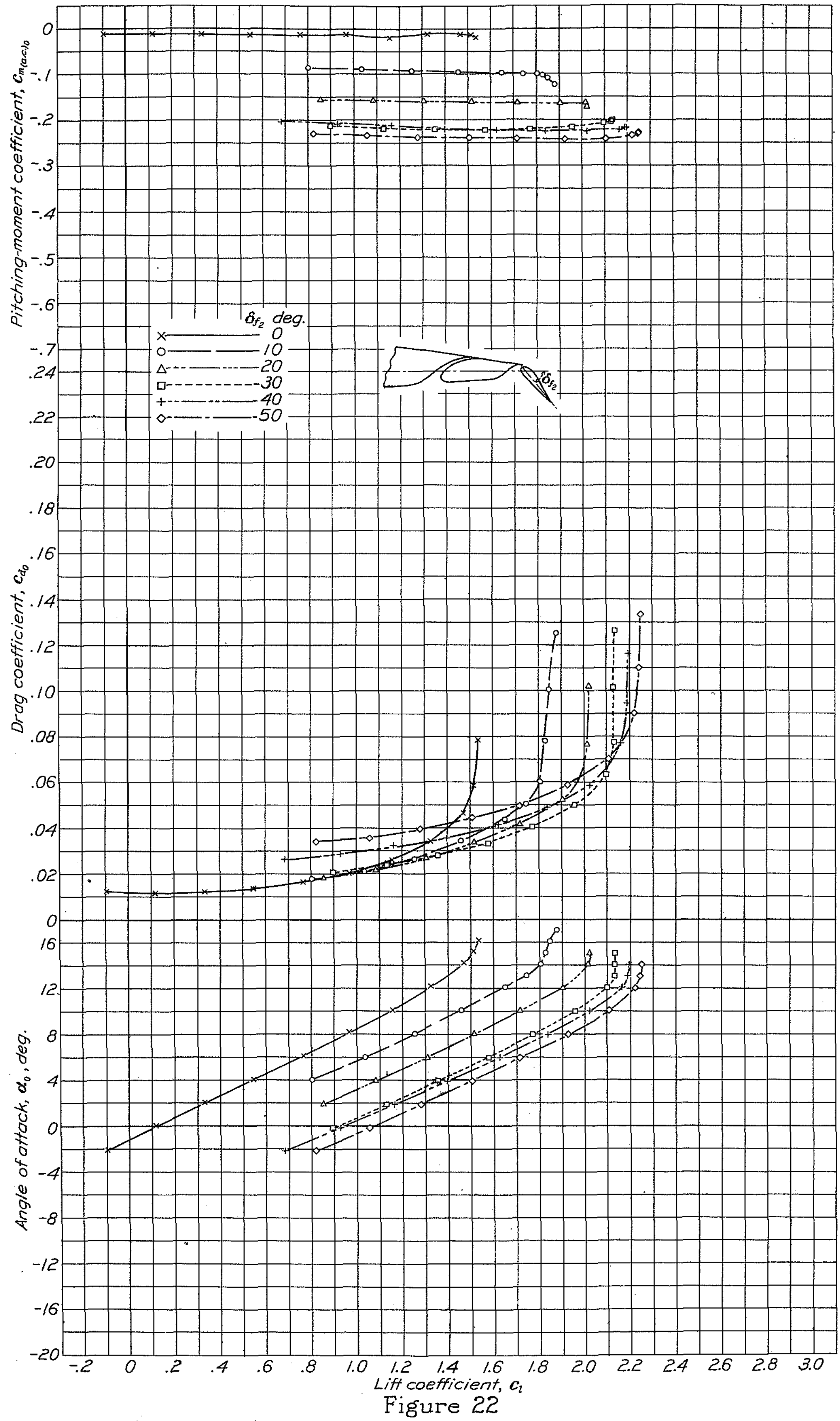

Pitching-moment coefficient, $c_{m_{(a.c.)_0}}$
Drag coefficient, c_{d_0}
Angle of attack, α_0, deg.
Lift coefficient, c_l
δ_{f_2} deg.
0
10
20
30
40
50
δ_{f_2}

Figure 22

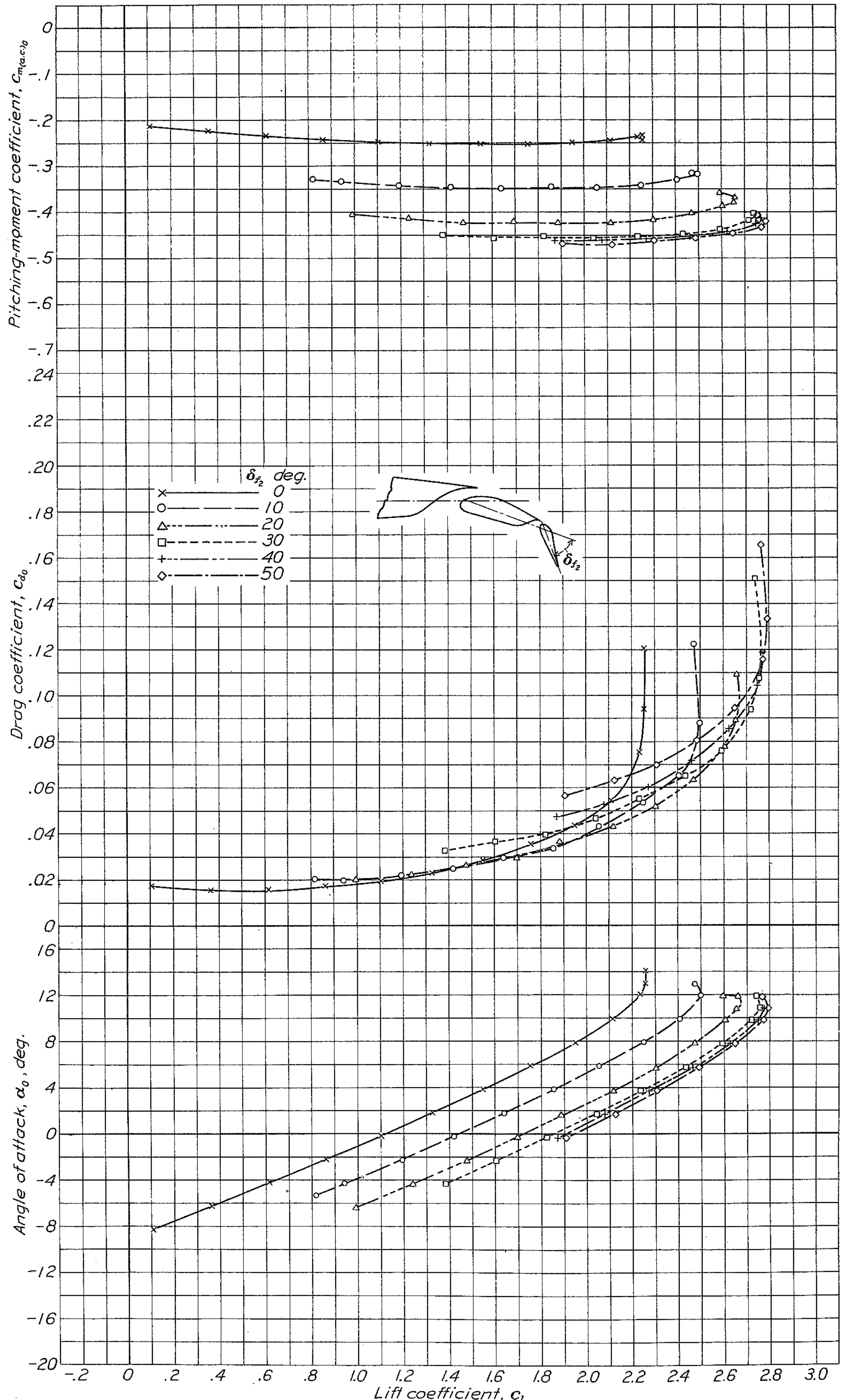
Pitching-moment coefficient, $c_{m_{(a.c.)_0}}$
Drag coefficient, c_{d_0}
Angle of attack, α_0, deg.
Lift coefficient, c_l
δ_{f_2} deg.
0
10
20
30
40
50
δ_{f_2}

Figure 23

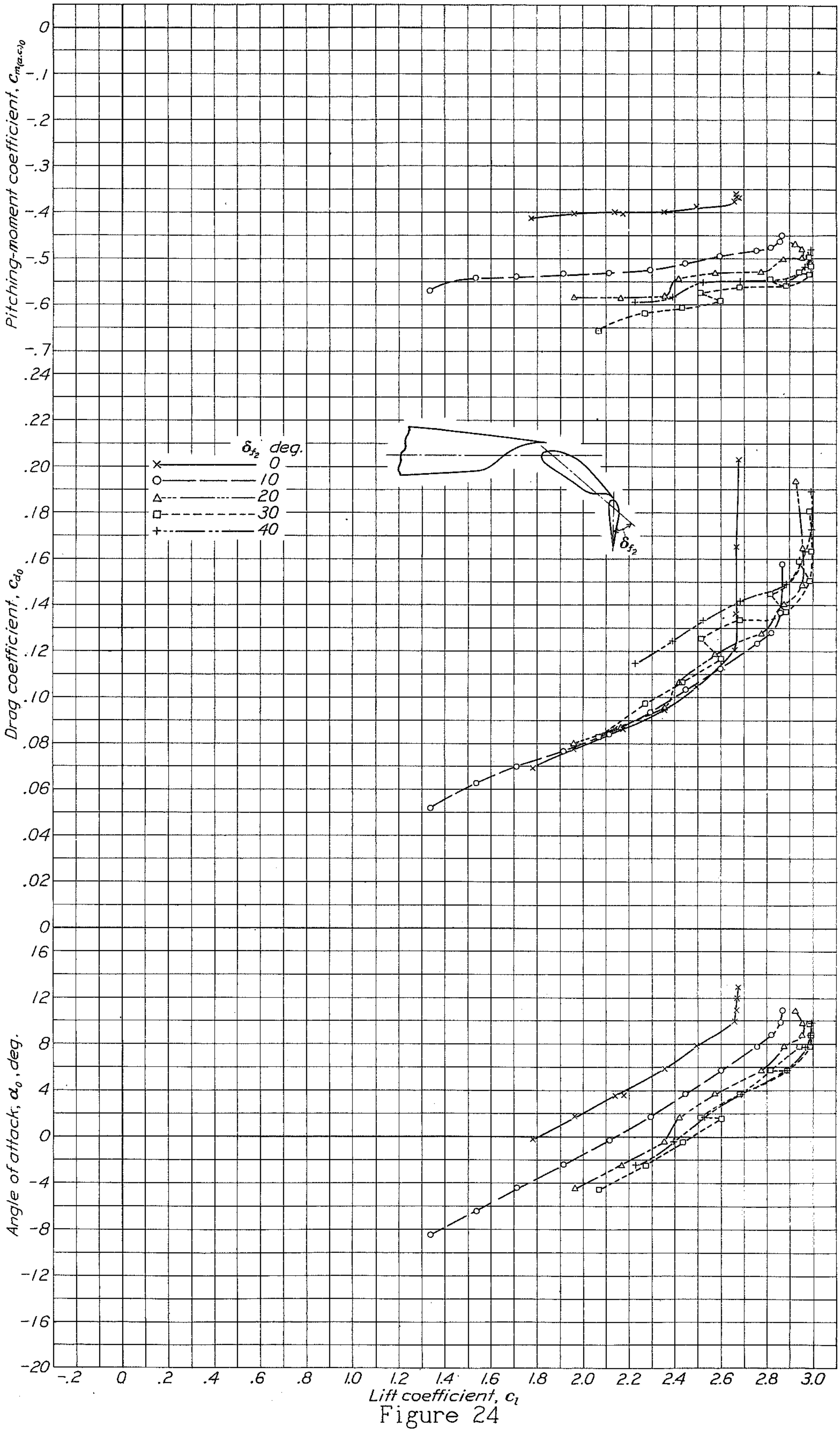
Pitching-moment coefficient, $c_{m(a.c.)_0}$
Drag coefficient, c_{d_0}
Angle of attack, α_0, deg.
Lift coefficient, c_l
δ_{f_2} deg.
0
10
20
30
40
δ_{f_2}

Figure 24

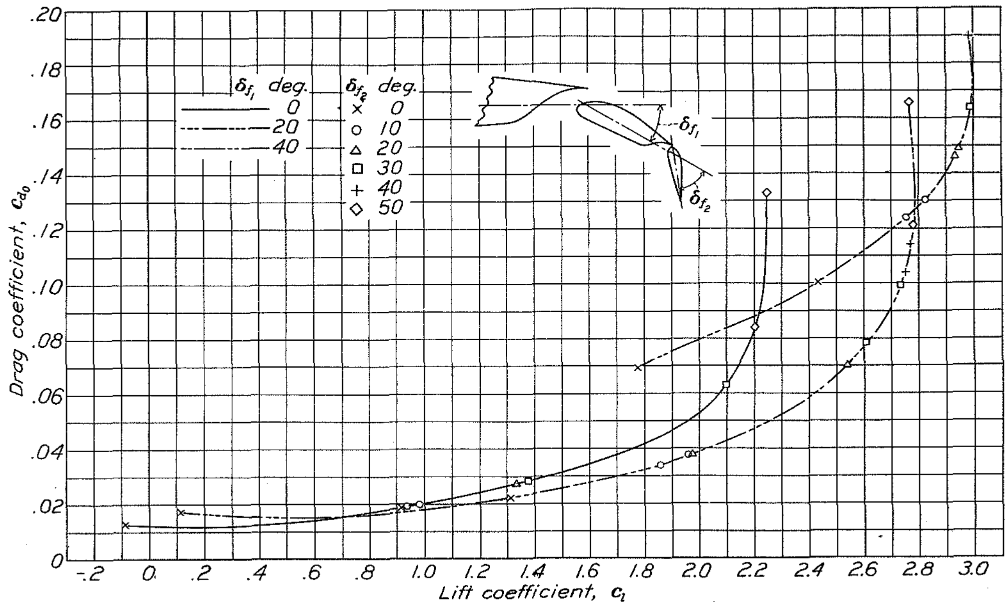

Figure 25

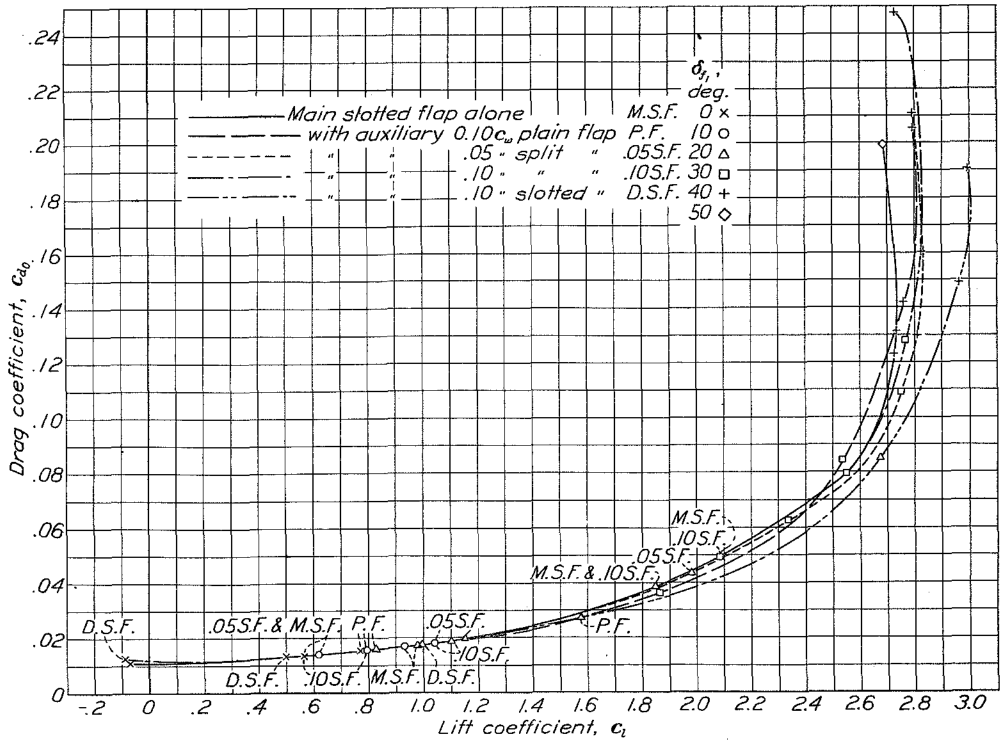

Figure 26